Published in final edited form as:
*Pain*. 2012 September ; 153(9): 1871–1882. doi:10.1016/j.pain.2012.05.028.

# Increasing TNF Levels Solely in the Rat Hippocampus Produces Persistent Pain-like Symptoms

**Regina T. Martuscello**[1,*,‡], **Robert N. Spengler**[2,‡], **Adela C. Bonoiu**[3], **Bruce A. Davidson**[1,4,5], **Jadwiga Helinski**[4,5], **Hong Ding**[3], **Supriya Mahajan**[6], **Rajiv Kumar**[3], **Earl J. Bergey**[3,7], **Paul R. Knight**[3,4,5,8], **Paras N. Prasad**[3,7], and **Tracey A. Ignatowski**[1,2,9,**,‡]

[1]Department of Pathology and Anatomical Sciences, School of Medicine and Biomedical Sciences, New York 14228

[2]NanoAxis, LLC, Amherst, New York 14228

[3]Institute for Lasers, Photonics, and Biophotonics, State University of New York at Buffalo 3435 Main Street Buffalo, NY 14214

[4]Department of Anesthesiology, School of Medicine and Biomedical Sciences, State University of New York at Buffalo 3435 Main Street Buffalo, NY 14214

[5]Veterans Administration Western New York Healthcare System, State University of New York at Buffalo 3435 Main Street Buffalo, NY 14214

[6]Department of Medicine, Division of Allergy, Immunology, and Rheumatology, School of Medicine and Biomedical Sciences, State University of New York at Buffalo 3435 Main Street Buffalo, NY 14214

[7]Department of Chemistry, School of Arts and Sciences, State University of New York at Buffalo 3435 Main Street Buffalo, NY 14214

[8]Department of Microbiology and Immunology, School of Medicine and Biomedical Sciences, State University of New York at Buffalo 3435 Main Street Buffalo, NY 14214

[9]Program for Neuroscience, School of Medicine and Biomedical Sciences, State University of New York at Buffalo 3435 Main Street Buffalo, NY 14214

## Abstract

The manifestation of chronic, neuropathic pain includes elevated levels of the cytokine tumor necrosis factor-alpha (TNF). Previously, we have shown that the hippocampus, an area of the brain most notable for its role in learning and memory formation, plays a fundamental role in pain sensation. Using an animal model of peripheral neuropathic pain, we have demonstrated that



** Corresponding author: Tracey A. Ignatowski, Ph.D. Research Associate Professor Department of Pathology and Anatomical Sciences School of Medicine and Biomedical Sciences University at Buffalo, The State University of New York 206 Farber Hall 3435 Main Street Buffalo, New York 14214 Tel: 716-829-3102; Fax: 716-829-2086; tai1@buffalo.edu.

*In partial fulfillment of the requirements for the Master of Arts degree, Department of Pathology and Anatomical Sciences, University at Buffalo, State University of New York

‡Authors contributed equally to writing of the manuscript.



Conflict of interest statement
The authors declare no conflict of interest concerning the present study.

intracerebroventricular (icv) infusion of a TNF antibody adjacent to the hippocampus completely alleviated pain. Furthermore, icv infusion of rTNF adjacent to the hippocampus induced pain behavior in naïve animals similar to that expressed during a model of neuropathic pain. These data support our premise that enhanced production of hippocampal-TNF is integral in pain sensation. In the present study, TNF gene expression was induced exclusively in the hippocampus eliciting increased local bioactive TNF levels, and animals were assessed for pain behaviors. Male, Sprague-Dawley rats received stereotaxic injection of gold nanorod (GNR)-complexed cDNA (control or TNF) plasmids (nanoplasmidexes), and pain responses (i.e., thermal hyperalgesia and mechanical allodynia) were measured. Animals receiving hippocampal microinjection of TNF nanoplasmidexes developed thermal hyperalgesia bilaterally. Sensitivity to mechanical stimulation also developed bilaterally in the rat hind paws. In support of these behavioral findings, immunoreactive staining for TNF, bioactive levels of TNF, and levels of TNF mRNA as per PCR analysis were assessed in several brain regions and found to be increased only in the hippocampus. These findings indicate that the specific elevation of TNF in the hippocampus is not a consequence of pain, but in fact induces these behaviors/symptoms.

## 1. Introduction

Pain is a sensation, as well as a perception involving cognition that integrates awareness with emotional responses and memory. The positioning of the hippocampus facilitates processing of direct and indirect nociceptive inputs of pain. The indirect nociceptive inputs from the periphery innervate the hippocampus through the spinothalamic and parabrachial ascending pathways [27], while septo-hippocampal neurons receive direct input from the spinal cord [17,28,42]. The hippocampus is connected to the parabrachial or thalamic regions through neuronal networks that modulate spinal nociceptive processing through activation of descending monoaminergic pathways from the brain stem [26,72].

The proximal pleiotropic cytokine tumor necrosis factor-alpha (TNF) is involved at all levels of the neuroaxis in the pathogenesis of chronic pain and is an integral determinant/component of nociception [19,20,22,37,39,48,53,61,64-66,73,74,76,79]. TNF is essential to the cognitive experience of pain and associated mood changes related to chronic pain. Concomitant with peripheral nerve injury in the sciatic nerve chronic constriction injury (CCI) model, hippocampal noradrenergic neurotransmission is dampened following elevated levels of hippocampus-TNF [19,37]. TNF-regulated release of brain norepinephrine is dependent upon $\alpha_2$-adrenergic receptor activation [40], and the presynaptic $\alpha_2$-adrenergic receptor is a principle regulator of norepinephrine release [69]. There is a correlation between $\alpha_2$-adrenergic receptor inhibition of norepinephrine release and upregulated levels of brain-TNF during neuropathic pain [19]. Therefore, it is not surprising that tricyclic antidepressant drug alleviation of pain correlates with enhanced norepinephrine release in the hippocampus following intra-peritoneal administration [39,40]. Alleviation of chronic pain by antidepressants involves an increase of monoamine neurotransmitter availability for neurogenesis [60], and the prevention and/or reversal of hippocampal volume loss [10,36]. Our data indicate that antidepressant-induced analgesia is mediated by the inhibition of TNF production [39,70,71]. Furthermore, intracerebroventricular (icv) microinfusion of recombinant TNF adjacent to the hippocampus produces pain behavior in the absence of any peripheral injury, implicating the hippocampus as a site of TNF's nociceptive action within the CNS [20,37,49]. We hypothesize that the sustained elevated levels of TNF limited to the hippocampus induce pain behaviors. Consequently, we designed a protocol that applies nanotechnology and gene transfection to enhance TNF production specifically in the hippocampus.

Gold nanorods (GNRs) and nanoparticles are used as delivery platforms *in vivo* and *in vitro* because of their low toxicity [18,35,57,77] and their non-immunogenic properties [6]. Previously, we used GNRs coated with cationic polyelectrolytes to deliver siRNA to silence the expression of glyceraldehyde 3-phosphate dehydrogenase in the hippocampus [7]. In the present study, we complexed cDNA plasmids that produce red fluorescent protein (RFP)-TNF fusion protein (GNR-pTag*rfp*-Mu*tnf* complexes, or TNF nanoplasmidexes) with GNRs, as "naked" plasmids exhibit poor cellular uptake, thereby offering protection and facilitating delivery to target cells. Since anti-nociception is elicited by decreasing hippocampus-TNF [20,37], it follows that elevated levels of TNF mediate the development of pain behaviors. Therefore, we stereotaxically injected TNF nanoplasmidexes into the CA1 region of the rat hippocampus and assessed the development of thermal hyperalgesia and mechanical allodynia. The nanoplasmidex-induced enhancement of bioactive TNF, TNF mRNA, and TNF-immunoreactive staining was assessed in various brain regions.

## 2. Materials and methods

### 2.1. Nanoplasmidex materials

Cetyltrimethylammonium bromide (CTAB), hydrogen tetrachloroaurate(III) trihydrate ($HAuCl_4{\cdot}3H_2O$), silver nitrate ($AgNO_3$), L-ascorbic acid, glutaraldehyde (50% aqueous solution), and sodium borohydride were purchased from Aldrich, and HPLC-grade water was used in all the experiments. Stock solutions of sodium borohydride and L-ascorbic acid were freshly prepared for each new set of experiments. Poly(3,4-ethylenedioxythiophene)/ poly(styrenesulfate) (PEDT/PSS, molecular weight 240,000) and poly(diallyldimethyl ammonium chloride) (PDDAC, 20%) were obtained from Polysciences, Inc.

### 2.2. Nanoplasmidex synthesis

The gene carriers were prepared using a seed mediated growth method described by Ding, *et al.* 2007. The GNR surface was prepared for DNA plasmid loading by adding two successive polymer layers of polyelectrolytes, PEDT/PSS (20%) for negative charge and PDDAC (20%) for positive charge. The detailed procedures in each step have been described [24,78]. The binding efficiency of plasmid DNA with GNRs was confirmed using agarose gel electrophoresis as described previously [7,8,13]. This data indicates that plasmid DNA complexed with GNRs, with the most efficient plasmid DNA loading of GNRs calculated to be 50 ng pDNA/μl of GNR. The nanoplasmidexes were prepared fresh before each experiment by incubating cDNA plasmid with GNR carrier (50 ng/μl) at room temperature for 10 min. The formation of nanoplasmidexes was confirmed by (a) surface charge measurements and (b) electrophoretic migrations under electric field. An important factor that dictates the behavior of GNRs is the surface charge or zeta potential [24]. Studies to examine nanoplasmidex surface charge were performed using a 90-Plus particle size analyzer (Brookhaven Instrument Corp) where the zeta potential was measured in the presence and absence of plasmid molecules. The experiments were performed at room temperature and the results were recorded after 4 measurements per sample. The zeta potential of the free GNRs used in these experiments was +25.71 mV, and upon successful complex formation to TNF plasmids, the zeta potential was reduced to -10.20 mV. Previous studies have shown that the zeta potential values influence the efficiency of GNR transfections, with slightly negatively charged complexes being more favorable [2,13,24]. Taken together, the combination of results in electrophoretic migration and charge determination confirmed the successful complex formation between GNRs and the Tag*rfp*-TNF pDNA constructs.

### 2.3. TNF-inducing plasmid

A plasmid encoding for a red fluorescent protein (RFP)-TNF fusion protein, TagRFP-MuTNF , was constructed by inserting the mouse *tnf* coding sequence into the mammalian expression vector, pTag*rfp*-C (Evrogen, Axxora, San Diego, CA). Briefly, *E. coli* HB101/pMu*tnf* (a mouse *tnf*-encoding plasmid, $amp^R$, GenBank: M11731) was obtained from ATCC (Manassas, VA). The mouse *tnf* coding sequence was amplified by PCR with primers to add restriction sites, EcoRI and BamHI, to the 5' and 3' ends, respectively (forward: 5'-CAGAAGGAATTCCATGAGCACAGAAAGC-3', reverse: 5'-ACACGCGGATCCTTCACAGAGCAATGAC-3'). Both the pTag*rfp*-C and Mu*tnf* PCR products were subjected to a combined EcoRI and BamHI restriction reaction and the resulting linear DNA products were ligated to generate the pTag*rfp*-Mu*tnf* fusion plasmid. The RFP-TNF fusion protein produced from the plasmid in a transfected eukaryotic cell is processed for TNF secretion by inserting into the plasma membrane with the TNF N-terminus head in the cellular ectodomain and the RFP C-terminus in the cytosol. Proteolytic cleavage at the plasma membrane-ectodomain boundary releases the TNF extracellularly, and the RFP is retained within the cell.

A functioning fusion protein, TagRFP-MuTNF was determined by transfecting HeLa cells with plasmid using FuGENE® HD (Roche Diagnostics, Indianapolis, IN) and assessing RFP production with fluorescence microscopy (see below). Culture supernatants and cell lysate preparations were assayed for TNF bioactivity. Transfection of these cells with pTag*rfp*-C served as the TNF bioactivity negative control.

### 2.4. Cell cultures

HeLa cells (ATCC, Manassas, VA) were cultured in DMEM + penicillin and streptomycin + amphotericin B + 10% heat-inactivated fetal bovine serum (Invitrogen, Chicago, IL) in T75 flasks at 37°C, 95% RH, 5% $CO_2$.

WEHI-13VAR fibroblast cells, a TNF-sensitive cell line derived from a mouse fibrosarcoma (ATCC, Manassas, VA), were grown in culture medium containing: RPMI-1640, 2 mM L-glutamine, 10% heat-inactivated fetal bovine serum (Invitrogen, Chicago, IL), and 3 μg/ml gentamicin (Sigma-Aldrich Chemical, St. Louis, MO) in T75 flasks at 37°C, 95% RH, 5% $CO_2$. Cells used in the TNF bioassay were always below passage 25 to avoid loss of TNF sensitivity.

### 2.5. In vitro assessment of pTagrfp-Mutnf to produce functioning protein

HeLa cells were grown to 80 - 90% confluency then seeded into 35 mm glass bottom culture dishes with a 10 mm #1.5 glass microwell (MatTek, Ashland, MA) or a 6-well plastic culture plate at $1.5 \times 10^5$ cells/dish (well) in 2 ml HeLa cell culture medium. After growing to 50-80% confluency, the cells were washed 2X with Opti-MEM® (Invitrogen, Chicago, IL), 1 ml Opti-MEM® was added, and the cells were incubated for 1 hr at 37°C, 95% RH, 5% $CO_2$. The transfection complex was prepared by combining 4 μl of 500 ng/μl appropriate plasmid DNA in $H_2O$ with 8 μl FuGENE HD® and 100 μl Opti-MEM®, vortexing briefly, and incubating at room temperature for 20 min. The entire volume of transfection complex was added to the appropriate dishes (wells) and incubated, as above, for another 4 hr. The transfection medium was replaced with 2 ml HeLa culture medium and incubated, as above, for 72 hr.

For assessment of TNF production, the culture medium was collected from the wells of the multiwell plate and centrifuged for 5 min at 400 × g at 4°C and the cell-free supernatant stored at -80°C. The attached cells were scraped into 0.5 ml buffer containing: 15 mM Tris, 150 mM NaCl, 1 mM $CaCl_2$, 1 mM $MgCl_2$, pH =7.4, and 1X protease inhibitor cocktail

(500 μM AEBSF HCl, 150 nM aprotinin, 1 μM E-64, 0.5 mM EDTA disodium, 1 μM leupeptin hemisulfate, EMD Chemicals, Gibbstown, NJ). The cells were sonicated on ice for 10 sec on 50% duty cycle (Sonifier Cell Disruptor 350 with microtip probe, Branson Ultrasonics, Danbury, CT) and the resultant sonicate transferred to a microfuge tube and stored at -80°C. The cell-free and cell-associated samples were assayed for TNF bioactivity.

For assessment of RFP fluorescence, the glass bottom culture dishes were observed with a Zeiss AxioObserver Apotome fluorescence microscope with 63X/1.4 PlanApo oil objective (Carl Zeiss MicroImaging, Thornwood, NY) equipped with a dsRed filter cube (ex filter, dichroic mirror, em filter: BP550/25, FT570, BP605/70). Representative photomicrographs were acquired using an AxioCam MrM cooled CCD camera and AxioVision v.4.8 image acquisition software (Carl Zeiss MicroImaging, Thornwood, NY) with all illumination and exposure settings the same for all samples.

### 2.6. TNF bioassay

The WEHI-13VAR fibroblast cell line that is sensitive to the lytic effects of TNF [41] was used to analyze extracts derived from brain tissue homogenates for the presence of biologically active TNF [40] with modification. Briefly, animals were euthanized by rapid decapitation and the locus coeruleus, the right and left hippocampi, and the parietal cortex, used as a control region, were isolated on ice for assay. Supernatants from homogenates centrifuged at 14,000 × g (15 min at 4°C) were stored at -80°C until analyzed for bioactive TNF. In addition, samples from HeLa cells transfected with the control and TNF-producing plasmid DNA were also analyzed. Briefly, WEHI-13VAR cells were cultured to approximately 90% confluency in culture medium as described above. Cells were prepared for the assay by detaching with 0.25% trypsin and 0.02% EDTA (Sigma-Aldrich Chemical, St. Louis, MO), adding 10 ml/flask culture medium, centrifuging at 800 × g for 5 min at RT, and resuspending in culture medium supplemented with 1 μg/ml actinomycin D (Calbiochem, La Jolla, CA) to a concentration of 500,000 cells/ml. One hundred microliters of cell suspension was added to each well of a flat-bottom 96-well tissue culture plate containing 100 μl of 2-fold serial dilutions of unknown samples, in triplicate, or known concentrations of rat recombinant TNF (for tissue sample analyses) or human recombinant TNF (for HeLa cell analyses) standards (R&D Systems, Minneapolis, MN) in diluting medium, RPMI-1640, 2 mM L-glutamine, 1% heat-inactivated fetal bovine serum, and 15 mM HEPES (Sigma-Aldrich Chemical, St. Louis, MO). Following 20 hr of incubation at 37°C, 95% RH, 5% $CO_2$, 10 μl of Cell Proliferation Reagent WST-1 (a solution of the tetrazolium salt, WST-1 (4-[3-(4-iodophenyl)-2-(4-nitrophenyl)-2H-5-tetrazolio]-1,3-benzene disulfonate and the electron coupling reagent, mPMS (1-methoxy-5-methyl-phenazinium methyl sulfate), Roche Diagnostics, Indianapolis, IN) in diluting medium was added to each well. After incubating for 4 hr at 37°C, 95% RH, 5% $CO_2$, the absorbance at 440 and 700 nm was measured using a SpectraMax 190 microplate reader with SoftMax Pro v.4.0 acquisition and analysis software (MDS Analytical Technologies, Sunnyvale, CA). A standard curve (0.01 pg/ml – 10,000 pg/ml, reverse sigmoid in shape) of the ($OD_{440}$-$OD_{700}$) vs log[TNF] was plotted and the [TNF] of each sample was determined from the dilution closest to the inflection point of the standard curve. This assay has a detection limit of approximately 1 pg/ml [31]. The assay is based on the specific cytotoxicity of the WEHI-13VAR cells to TNF in the presence of actinomycin D. WST-1 counting solution was used as a cell viability indicator, which is quantitated spectrophotometrically [5]. Increasing TNF concentration results in increased cell death and, therefore, a reduced absorbance at 440 nm. Results are expressed as the percentage of control values (pg/100 mg tissue weight) for the brain tissue samples and pg/ml for the HeLa cell samples.

### 2.7. Animals

Male, Sprague-Dawley rats (Harlan Sprague Dawley Inc., Indianapolis, IN) initially weighting 200-230 g were used for all experiments. The rats were housed in single cages at 23 ± 1 °C in Laboratory Animal Facility–accredited pathogen-free quarters with *ad libitum* access to food and water. The animals were maintained on a 12 h light/dark cycle with the lights on from 0600 to 1800 h. Rats were given at least 3 days to acclimate to the animal facilities before baseline testing occurred. All experiments were carried out in concord with protocols approved by the Institutional Animal Care and Use Committee (IACUC) of The University at Buffalo, as well as in accordance with the guidelines for the ethical treatment of animals established by the National Institute of Health and the Committee for Research and Ethical Issues of IASP [80]. All efforts were used to ensure animal safety and minimal animal suffering, as well as the use of only enough animals to guarantee statistical accuracy.

### 2.8. Intra-hippocampal injection

Animals were anesthetized with an i.p. injection of ketamine (75 mg/kg) and xylazine (10 mg/kg) and secured on a stereotaxic platform. Coordinates: A-P, -3.3 mm relative to bregma; lateral, 1.6 mm relative to the midline; depth, -2.8 mm from dura were used for microinjection into the CA1 region of the hippocampus [51]. TNF nanoplasmidexes or control nanoplasmidexes were bilaterally injected into the CA1 region of the hippocampi. GNRs alone were not injected due to a difference in surface charge as compared to the nanoplasmidexes [7,8], and therefore are not an appropriate control. The concentration of nanoplasmidexes (150 ng in 3 μl) for injection was based on both *in vitro* and *in vivo* studies. Each injection was at a rate of 0.5 μl/min using a 30 G stainless steel needle on a 10 μl Hamilton syringe, held by the micromanipulator on the stereotaxic apparatus [43]. The needle remained in place for another 3 minutes after each injection to allow for sufficient diffusion. Authentication of the injection site was established by gross morphology of the hippocampus at dissection.

### 2.9. Thermal hyperalgesia measurements

Hyperalgesia (increased reaction to painful sensory stimuli) was measured by determining changes in hind paw withdrawal latency using a plantar algesia apparatus [34]. Paw withdrawal was measured using an intense heat source to stimulate thermal receptors in the sole of the foot. A maximum automatic cut-off time of 15s was used to prevent tissue damage. Rats were placed in Plexiglas chambers, on top of a temperature regulated (32 ± 0.1 °C) glass surface. Rats were acclimated to this testing apparatus for 7-10 minutes prior to testing, and measurements of the thermal withdrawal were taken for the left and right hind paws. Baseline tendencies were determined for 3 days before experimental treatment for all animals and expressed as the mean values of three separate trials. Paw withdrawal responses were measured every other day alternating one day post-surgery for a 21 day period. Only rapid hind paw withdrawal movements were considered as a reaction response to the thermal stimulus; weight shifting or normal movement within the Plexiglas boxes were not considered significant movements. Each hind paw was measured three times at an interval of ≥ 4 min. All measurements were recorded between 0800 and 1200 hours.

### 2.10. Mechanical allodynia measurements

Mechanical allodynia was determined by measuring the hind paw withdrawal threshold in response to stimuli from von Frey filaments [14]. Rats were placed in a wire-mesh raised cage and were acclimated for 7-10 min (or until exploratory behavior ceased). Calibrated filaments were applied to the plantar surface of the hind paws and paw withdrawal reflexes were recorded for each hind paw. The criterion response is reflexive withdrawal without stepping. A series of von Frey hairs was applied to the central region of the plantar surface

in ascending order. Each hind paw was measured two times with brief probes at ≥ 1 min intervals. If withdrawal did not occur, the next larger filament was applied. When the hind paw was withdrawn from a filament, the value of that filament (grams) was the withdrawal threshold. The differential response between the baseline and post-surgery values for each hind paw is a measure of tactile allodynia. Individual paw withdrawal threshold was determined by 3 days of baseline testing performed between 0800 h and 1200 h. Paw withdrawal responses were measured every other day alternating one day post-surgery for a 21 day period. Regular movement and inadvertent movements were not considered as a direct response to the filament application.

### 2.11. Immunohistochemistry for TNF

Upon decapitation, the hippocampi were harvested. The left hippocampus was processed for either TNF bioassay or PCR analysis for TNF mRNA. The right hippocampus was embedded in Tissue-Tek® OCT compound (Finetech, Torrence, CA), snap frozen in liquid nitrogen and processed for immunohistochemistry. Cryostat sections (4-6 μm) of harvested tissues were serially cut and collected on StarFrost™ glass slides (Mercedes Medical, Sarasota, FL). Sections were fixed with acetone (15 min), fan-dried (30 min) and stained for TNF according to previously published protocols [38] with the following changes: Sections were incubated with 10% goat serum in PBS supplemented with 0.1% BSA (MP Biomedicals Inc., Irvine, CA) for 30 minutes to block non-specific binding. Goat serum was dripped off of the slides, and sections incubated with the primary antibody, polyclonal rabbit anti-mouse TNF (Calbiochem-Novabiochem, La Jolla, CA) that cross-reacts with rat TNF, at 1:200 dilution (in PBS supplemented with 0.1% BSA) for 1 h. Following two PBS rinses, biotinylated goat anti-rabbit secondary antibody (Vectastain kit, Vector Labs, Burlingame, CA), preabsorbed (1:100 dilution) in normal rat serum at 37 °C for 45 min prior to use, was added to sections and incubated for 45 minutes. Slides were rinsed in PBS, incubated with biotinylated enzyme conjugate (Vector) for 30 min, and the reaction localized using 3,3'-Diaminobenzidine (DAB) substrate for 5 min. SIGMA FAST™ DAB tablets were dissolved in 0.05 M Tris supplemented with 0.01 M imidazole. Rinsing with distilled water (two rinses, 5 min each) terminated the development of color. Unless stated otherwise, all incubations were carried out at room temperature. As a negative control, primary antibody was substituted by normal rabbit serum at the same protein concentration, which did not result in any specific labeling.

### 2.12. Quantitative analysis of TNF immunoreactive staining

As previously published, images from stained tissue sections were captured under bright-field conditions using a digital camera (Pixera 600ES-CU) attached to a Zeiss Axiovert 35 microscope and using imaging device Viewfinder (version 3.0.1; Pixera Corp.) and Studio (version 3.0.1; Pixera Corp.) software [71]. Images from paired animals were obtained on the same day using the same light intensity and magnification (200X or 400X) settings by one observer who was not aware of the treatment groups. Images were saved as tiff files and analyzed using ImageJ 1.32j software (NIH, USA, http://rsb.info.nih.gov/ij/) with the Color Deconvolution plug-in to perform stain separation. Following background subtraction, color deconvolution of the RGB tiff files was performed using the built-in hematoxylin and DAB (H DAB) vector, as the third (complementary) 8-bit image generated was completely white [58]. The second 8-bit tiff file corresponding to the DAB (TNF) contribution was then further analyzed. This 8-bit tiff file was converted to grey-scale and thresholded in ImageJ using the auto threshold tool. Resultant mean density values for TNF staining were compared.

Confocal microscopic images were obtained using a spectral confocal microscope (TCS SP2, Leica Microsystems Semiconductor GmbH) with a HXC PL APO CS 63.0x1.40 oil immersion objective.

### 2.13. Immunofluorescent staining

Hippocampal sections on slides stored at -30°C in the dark were brought to room temperature and fixed in acetone, 10 min at room temperature. Slides were completely dried prior to hydration in 1X PBS at room temperature, 3 times, 5 min each. Immunofluorescence staining procedures were followed as previously published [7]. Briefly, non-specific immunoglobulin binding was blocked with 10% goat serum for 20 min at room temperature. Slides were blotted without washing to remove serum. Sections were incubated with primary antibody for either glial fibrillary acidic protein, mouse monoclonal anti-GFAP (1:30,000, Sigma-Aldrich) or neurofilament-200, mouse monoclonal NF-200 (1:30,000, Sigma-Aldrich), both of which cross-react with rat, 120 min, in 1X PBS/1% bovine serum albumin (BSA) (fraction V)/10% goat serum at room temperature in a humidified chamber in the dark. Slides were washed 3 times, 5 min each, in 1X PBS. Sections were incubated with the secondary antibody, goat anti-mouse IgG1-AlexaFluor 647 (1:2,000, Invitrogen), in 1X PBS/1% BSA, 120 min at room temperature in a humidified chamber in the dark. Slides were washed 5 times, 5 min each, in 1X PBS. Sections were incubated with Hoechst nuclear stain (10 M) for 1 min. Slides were rinsed with 1X PBS, 1 time, 5 min. Fluoromount aqueous mounting medium with anti-fade properties (Sigma) was added to slides, which were then cover slipped and edges sealed with Cytoseal™-60 (Thermo Scientific). Slides were stored in the dark at 4°C until analyzed. Fluorescence images were obtained with a Zeiss Axio Imager Z1 fluorescence microscopy system with 20X objective (Carl Zeiss MicroImaging, Thornwood, NY). Representative photomicrographs were acquired using an AxioCam MrM cooled CCD camera and AxioVision v.4.8 image acquisition software (Carl Zeiss MicroImaging, Thornwood, NY) with constant illumination and exposure settings.

### 2.13. PCR analysis

Upon dissection, the CA1 region and the CA3/dentate gyrus portion of the hippocampus, as well as a portion of the parietal cortex directly over the site of hippocampal injection, were each placed into 1 ml RNA*later* solution (Ambion) and stored at -80°C until RNA extraction. Total RNA was extracted by an acid guanidinium-thiocynate-phenol-chloroform method as described using TRIzol reagent (Invitrogen-Life Technologies, Carlsbad, CA) [15]; brain tissue samples were processed as published [7,8]. RNA concentrations were determined using a Nano-Drop ND-1000 spectrophotometer. Isolated RNA was stored at –80°C.

Quantitative real-time PCR (qRT-PCR) was used to quantitate the relative abundance of each mRNA species using specific primers for rat TNF-α: Forward primer: 5’-TACTGAACTTCGGGGTGATTGGTCC-3’ and reverse primer: 5’-CAGCCTTGTCCCTTGAAGAGAACC-3’. These sequence data are available from GenBank under accession number X66539. RNA was reverse transcribed to cDNA using a reverse transcriptase kit (Promega Inc, Madison, WI). Relative abundance of each mRNA species was quantitated by q-PCR using specific primers (Maxim Biotech, Inc., Rockville, MD) for TNF and -actin (GenBank Accession number X00351) using the Brilliant® SYBR® green q-PCR master mix (Stratagene Inc, La Jolla, CA). Relative expression of mRNA species was calculated using the comparative $C_T$ method [11,52]. All data were controlled for quantity of RNA input by performing measurements on an endogenous reference gene, -actin. Results on RNA from treated samples were normalized to results obtained on RNA from the control sample. Briefly, the analysis was performed as follows: for each sample, a difference in $C_T$ values ($\Delta C_T$) was calculated for each mRNA by taking

the mean $C_T$ of duplicate tubes and subtracting the mean $C_T$ of the duplicate tubes for the reference RNA ( -actin) measured on an aliquot from the same RT reaction. The $C_T$ for the treated sample was then subtracted from the $\Delta C_T$ for the control sample to generate a $\Delta\Delta C_T$. The mean of these $\Delta\Delta C_T$ measurements was then used to calculate expression of the test gene relative to the reference gene and normalized to the control as follows: Relative Expression/Transcript Accumulation Index = $2^{-\Delta\Delta CT}$. This calculation assumes that all PCR reactions are working with 100% efficiency. All PCR efficiencies were found to be >95%; therefore, this assumption introduces minimal error into the calculations. Data are the mean ± SD of 3 separate experiments done in duplicate. Statistical significance was determined using Student's *t*-test based on comparisons between TNF nanoplasmidexes and control nanoplasmidexes.

### 2.14. Statistics

All results are expressed as mean values S.E.M. Analysis of data was performed using SigmaStat statistical software (SPSS Inc., Chicago, IL). Data were analyzed using Student's *t*-test, Paired *t*-test, Mann-Whitney Rank Sum test, or Kruskal-Wallis ANOVA on Ranks and Dunn's post-hoc test. A difference was accepted as significant when $p < 0.05$.

## 3. Results

### 3.1. In vitro assessment of pTagrfp-Mutnf function by cell culture transfection

Constructed plasmid production of functioning fusion protein, TagRFP-MuTNF, in eukaryotic cells was determined by transfecting HeLa cells with plasmids using FuGENE® HD (Roche Diagnostics, Indianapolis, IN) and assessing RFP production with fluorescence microscopy. Seventy-two hours following transfection, the pTag*rfp*-C (non-TNF producing control plasmid) transfected HeLa cells demonstrated homogenous cytosolic distribution of RFP fluorescence, whereas the pTag*rfp*-Mu*tnf* transfected cells demonstrated heterogenous, punctate fluorescence associated with the Golgi apparatus, vesicular packaging, and plasma membrane insertion of the RFP-MuTNF fusion protein (Figure 1). Fluorescence was not detected (autofluorescence) in non-transfected, control samples when acquired using the same illumination and camera settings as those used with the transfected samples. An identical pattern was seen in COS-1 cells (data not shown).

Culture supernatants and cell lysate preparations were assayed for the production of TNF bioactivity using a WEHI-cytotoxicity bioassay. Culture supernatants from pTag*rfp*-Mu*tnf* transfected HeLa cells had ≈ 5,700-fold higher levels of bioactive TNF than cells transfected with the pTag*rfp*-C plasmid control (3,510 ± 35.8 vs 0.61 ± 0.04 pg/ml, $p < 0.00001$, n = 3). Similarly, cell lysate preparations from the pTag*rfp*-Mu*tnf* transfected cells had ≈ 1,200-fold higher levels of bioactive TNF than the cells transfected with the pTag*rfp*-C plasmid control (668 ± 147 vs 0.55 ± 0.04 pg/ml, $p < 0.02$, n = 3).

### 3.2. Weight gain for nanoplasmidex injected animals

Rats microinjected bilaterally into the CA1 region of the hippocampus with the TNF nanoplasmidexes did not experience any difference in weight gain over time (three weeks) as compared to the paired control animals (data not shown). Weight was matched before surgery, and all rats maintained good health throughout the experimental period; no motor dysfunction was observed in rats receiving microinjection surgery.

### 3.3. Hind paw thermal hyperalgesia in TNF nanoplasmidex microinjected animals

In addition to decreasing depressive-like behavior, antidepressants have been shown to decrease levels of TNF in the brain [38,54,71]. These same drugs are also employed for the treatment of neuropathic pain. Therefore, we determined whether increasing localized

hippocampal TNF expression and consequently TNF bioactive levels would induce the expression of pain behaviors in rats. Animals were initially injected with 30 ng/3 μl of the nanoplasmidexes into the hippocampal CA1 regions. The animal receiving the TNF nanoplasmidexes did exhibit a slight thermal hyperalgesic response when observed over time in the pain behavioral assay (data not shown). These initial findings together with increased message for TNF in the hippocampus of an animal injected with the TNF nanoplasmidexes as compared to the control nanoplasmidexes encouraged further *in vivo* experiments using the TNF nanoplasmidexes. However, in order to induce a more robust behavioral response in the pain assays, the dosage was increased in subsequent animals to 150 ng/3 μl.

Sprague-Dawley rats (250–300 g) microinjected with 150 ng/3 μl TNF nanoplasmidexes bilaterally into the hippocampal CA1 region developed thermal hyperalgesia that was similar to that expressed by rats undergoing neuropathic pain in the CCI model [19,37,39]. Withdrawal latency for the right and the left hind paws (Figure 2A and B) demonstrated that TNF nanoplasmidexes injected into the CA1 hippocampal region induced hypersensitivity to a thermal stimulus for each hind paw. At day 12 (for the right paw) and day 16 (for the left paw) post-injection there was an increased sensitivity to thermal stimuli in the TNF nanoplasmidex-injected animals as compared to the control nanoplasmidex-injected animals. The increased sensitivity remained elevated throughout the time frame assessed (up to day-21 post-injection). Additionally, the control plasmid injected rats did not show any significant differences in withdrawal latency over time as compared to their respective hind paw baseline values, whereas withdrawal latencies were reduced upon thermal stimulation of the hind paws in the TNF plasmid injected rats (right hind paw baseline value = 13.14 ± 0.35 sec, post-microinjection day 16 = 10.77 ± 0.88 sec and day 20 = 10.49 ± 1.05 sec, $p < 0.05$, Paired *t*-test; left hind paw baseline value = 13.74 ± 0.28 sec, post-microinjection day 16 = 10.88 ± 1.18 sec, day 18 = 11.33 ± 0.98 sec, and day 20 = 10.98 ± 0.80 sec; $p < 0.05$, Paired *t*-test). These findings support the hypothesis that enhanced production of TNF in the hippocampus is sufficient for development of behavior indicative of chronic pain.

### 3.4. Mechanical allodynia in TNF nanoplasmidex-microinjected rats

Mechanical withdrawal thresholds were assessed for three weeks in animals receiving a one-time, bilateral microinjection of TNF nanoplasmidexes and those receiving control nanoplasmidexes into the CA1 region of both hippocampi. As presented in figure 3, mechanical withdrawal thresholds were significantly reduced in rats that were microinjected with the TNF nanoplasmidexes. Allodynia observed in both the right (Figure 3A) and left hind paws (Figure 3B) is sporadic and temporary in control nanoplasmidex microinjected rats, but is consistent and more robust within the TNF nanoplasmidex group beginning at day-12 post surgery.

### 3.5. Quantitative real time-PCR (qRT-PCR) analysis for TNF mRNA

Results from qRT-PCR analysis of brain tissue harvested from rats receiving intra-hippocampal CA1 injection of TNF nanoplasmidexes (150 ng/3 μl) display an increase in TNF mRNA expression (Figure 4A). Compared to values obtained after control nanoplasmidex injections, the TNF nanoplasmidexes induced an 85% increase in TNF mRNA expression in the CA1 region of the hippocampus (Figure 4A).

### 3.6. TNF bioassay

Results obtained from TNF bioassays show a significant increase in the bioactive levels of TNF in the hippocampus as compared to hippocampi from animals injected with the control nanoplasmidexes (Figure 4B). Hippocampal tissue homogenates prepared from pTag*rfp*-Mu*tnf* microinjected rats had ≈ 13-fold higher levels of bioactive TNF than homogenates

prepared from rats microinjected with the pTag*rfp*-C plasmid control (145 ± 58.5 pg/ml//100 mg tissue vs 11.2 ± 4.51 pg/ml/100 mg tissue, $p = 0.011$, Student's *t*-test). Furthermore, an increase in TNF does not occur in other areas of the brain investigated (Figure 4B). This confirms that TNF nanoplasmidexes were injected into the correct region of the brain and remain localized in the hippocampus without diffusing into other areas of the brain. Therefore, it can be concluded that while there are significantly higher amounts of TNF in the hippocampi from the TNF nanoplasmidex-injected animals, levels of TNF in the other areas of the brain that were assessed from the TNF nanoplasmidex-injected animals did not differ from the levels in animals receiving the control nanoplasmidexes.

### 3.7. RFP detection in hippocampal tissue sections

Figures 5a and 5b show the cellular uptake of nanoplasmidexes in hippocampal cells after stereotaxic injection into the CA1 region of hippocampus [51]. The nanoplasmidexes appear to remain localized to the CA1 region, with little diffusion to adjacent regions, as detection of RFP fluorescence is pronounced in the CA1 region when viewed across each of the coronal sections throughout the rostral half of the hippocampus [7]. These results confirm that stereotactic injection allows for localization of the nanoplasmidexes to desired/specific regions, as well as the uptake of the nanoplasmidexes into cells of the hippocampus.

### 3.8. Immunohistochemical staining for TNF in hippocampal tissue sections

Figure 5 shows sections from paired rats receiving (c) control or (d) TNF nanoplasmidex microinjection. It can be seen in panel d that the TNF nanoplasmidex-injected animal shows an increased amount of TNF in the cells. The brighter and more vibrant brown color in the surrounding tissue of this section is believed to indicate increased secretion of TNF in this area of the brain. The section prepared from the control animal (Figure 5c) show a lighter, purple color (hematoxylin) in the cells indicating lack of significant staining for TNF. Quantitative analysis of the hippocampal sections is presented in figure 6. Statistical analysis was achieved by analyzing staining in individual neurons ($n = 10$/section) and comparing staining results between the TNF nanoplasmidex and the control nanoplasmidex hippocampal sections. It can be seen that there is a higher concentration of TNF expressed in the sections from TNF nanoplasmidex-injected animals than in the control nanoplasmidex-injected animals with respect to integration density (sum of the values of the pixels in the selected image; equivalent to Area × Mean Gray Value) and the percent area (percentage of pixels in the selected image) of the individual neurons in the stained tissue. These findings suggest that the compartmentalization of TNF synthesis within neurons remains conserved to some extent since the area within the neuron that produces TNF does not increase that much (19.26% increase for TNF nanoplasmidex, Figure 6B), whereas the amount of TNF produced in the neuron is greatly increased (48.93% increase in integrated density values in TNF nanoplasmidex as compared to control nanoplasmidex, Figure 6A). These findings demonstrate that intra-hippocampal CA1 injection of TNF nanoplasmidexes induces a significant increase in staining for TNF in this brain region, with robust staining observed in neurons as identified by cell morphology.

### 3.9. Immunfluorescent staining for neurons and glial cells in hippocampal tissue sections

In an attempt to determine the cell type(s) in which the uptake of the nanoplasmidex was associated *in vivo*, rat coronal hippocampal sections were labeled with primary antibodies to either glial fibrillary acidic protein (GFAP) (glial cells) or neurofilament-200 (NF-200) (neurons) [7]. Visualization of the primary antibody labeling was achieved using an IgG1-AlexaFluor 647 (AF-647) secondary antibody, with the excitation/emission maxima at 650/668 nm. The nanoplasmidex-RFP uptake into hippocampal cells was visualized in the same tissue sections, since the excitation/emission maxima of 555/584 nm for RFP provides emission in the orange region of the spectrum and is well separated from the far-red

(AF-647) fluorophore emission, thereby facilitating a multicolor analysis. An overlay of the respective images (Figure 7, Rows A and B, panel c) demonstrates that co-localization of nanoplasmidexes may occur with either neuronal (NF-200 positive; Row A) or glial (GFAP positive; Row B) cells (Figure 7). Whereas the punctuate red staining together with the more diffuse RFP staining in Row A, panel b indicates production of TNF by neurons (NF-200 positive co-localization); the mainly diffuse RFP staining in Row B, panel b may indicate that the fusion protein has already been delivered to the glial cell (GFAP positive co-localization) plasma membrane, and the TNF released freeing the RFP to diffuse throughout the cytosol.

## 4. Discussion

Injury to peripheral nerves sends pain signals to the brain. If left unabated, the signals continue to be sent to the brain, which can essentially memorize the pain and become hypersensitive (central sensitization). Therefore, understanding the messengers involved in this process and the brain regions affected by this process is imperative for prevention of chronic pain development. Of particular interest, the hippocampal region plays an integral role in the perception of pain [27,28,30,42,47,63]. Peripheral nociception affects the hippocampus and induces biomolecular changes that helps further characterize the affective-cognitive aspects of pain, including the relationship between pain and mood, individual coping strategies, and formation of memories about painful stimuli [25]. Clinical reports estimate that over half of chronic pain patients also display characterized symptoms of clinical depression [29]. Yet, the importance of the emotional component of pain and its impact on the perception and cognition of pain has yet to be grasped by the pain-studying scientific community [25]. The central pain theory that explains the mechanisms of antidepressants that are involved in the inhibition of pain perception appears to be distinct from their antidepressant action, based on the observation that lower doses are effective in alleviating symptoms of chronic pain [1]. Inhibition of monoamine reuptake in the CNS [56], as well as activation of the opioid system [9,59] has been offered as a possible mechanism mediating antidepressant analgesia/anti-nociception. However, the finding that the phosphodiesterase inhibitor (rolipram) that is both an analgesic, as well as an antidepressant, does not directly affect neurotransmitter reuptake or the opioid system, but does suppress TNF production [32,33,67], supports the hypothesis that neuromodulators/neurotrophic factors mediate the anti-nociceptive action of antidepressants [39]. One such factor, TNF, is a pleiotropic cytokine produced by a plethora of cell types affecting numerous cellular functions. Although originally classified as a pro-inflammatory cytokine that regulates both innate and adaptive immune responses, it is now also recognized as a neuromodulator, regulating many neuron functions. In fact, both receptors for TNF (TNFR-1, p55TNFR and TNFR-2, p75TNFR) are constitutively expressed on all neuron cell types, but not on astrocytes and oligodendrocytes. Therefore, TNF does serve as a neuromodulator in the nervous system. This is supported by previous findings from our laboratory showing that: (1) TNF is produced in the brain, and specifically, in the hippocampus [19,20,38,68,71]; (2) antidepressants decrease TNF expression in the brain [38,71], which supports our premise that the over-expression of TNF mediates chronic pain; and (3) TNF inhibits norepinephrine release in the hippocampus [19,38,40,54,55]; thus, the lower level of norepinephrine that is linked to neuropathic pain may be explained by the greater inhibition of norepinephrine release due to enhanced production of TNF during this devastating disorder. Based on all of the above, it is plausible that enhanced TNF production contributes to the ongoing inflammatory cascade, synaptic dysfunction, and neuron death characteristic of neuropathic pain.

The hippocampus receives noradrenergic innervation exclusively from the locus coeruleus [44] and is involved in tonic pain perception [47]. Projections from the locus coeruleus to

the hippocampus: (a) are replete with terminals expressing presynaptic $\alpha_2$-adrenergic receptors; (b) contain $\alpha_2$-adrenergic receptors that mediate antidepressant therapeutic action; and (c) process painful stimuli [45]. Our selection of the CA1 region of the hippocampus for our microinjection experiments is based on the knowledge that neurons in this region respond to painful stimuli. Our lab has demonstrated that icv microinfusion of TNF into the right lateral cerebral ventricle adjacent to the hippocampus induces pain behavior [37,71]. Studies from other laboratories have confirmed that the hippocampal CA1 region and dentate gyrus are involved in neural processing related to persistent pain [63]. In addition, many clinical and basic research studies have shown hippocampal involvement in the action of antidepressant drugs [46,62]. These observations support the notion that the hippocampus is involved in the development and reoccurring effects of chronic pain.

TNF is involved in pain processing as established by assessing its levels systemically and/or peripherally and finding associations between the amount of TNF and disease severity/progression. We have assessed TNF levels in the brain during pain, especially considering the involvement of the hippocampus. Our past findings support an induction of TNF synthesis in the brain following peripheral chronic constriction injury [19,68]. However, from those studies, it could not be excluded that peripheral TNF might be transported into the CNS [4,50]. Whereas the effect of icv [37,49], systemic [21], or intraneural [73,79] application of TNF has been studied, we present for the first time a nociceptive effect of intra-hippocampal production of TNF. The present findings strongly support a direct role for TNF in the brain in the development of persistent pain behavior in the absence of peripheral nerve injury. Localized pathological changes during the development of chronic pain are evident in the hippocampus, which is also the most severely affected brain region resulting in hippocampal atrophy. By microinjecting TNF nanoplasmidexes that express RFP bilaterally into the CA1 region of naïve rats, we have confirmed the importance of the hippocampus in the development of pain. Rats developed peripheral hypersensitivity (Figures 2 and 3) concomitant with localized hippocampal increase in TNF (Figures 4-6) in the absence of injury. Whereas we have previously shown direct evidence for enhanced production of TNF in the hippocampus during a neuropathic pain model [19,71], we now demonstrate that TNF production alone in the hippocampus induces pain behavior. These data provide proof-of-principle that the hippocampus, a region involved in the emotional and cognitive components of pain, is integral in the development of chronic, persistent-like pain behaviors.

In order to support our hypothesis that states that enhanced TNF production limited to the hippocampus elicits pain symptoms similar to that observed during chronic pain models, we designed an effective and direct approach of nanoplasmidex delivery by bilateral CA1 microinjection. The success of our experimental approach allows for future studies delving into the complexities of the hippocampus including the analysis of unilateral injection effects. Some investigations demonstrated that various stimuli mediate bilateral effects in the hippocampus [3,12,16,27,75], while other investigations showed a unilateral or specific hippocampal effect following noxious stimuli [23,70]. In regards to the present study, previous investigations showed that alterations in the hippocampus have been detected following the onset of persistent inflammatory pain [27]. This observation leads to a fundamental question: whether the changes in the hippocampus are a consequence of the perception of pain or, as proposed in previous studies where enhanced hippocampal TNF production occurs during chronic pain [20,37,70,71], elicits the pain symptoms. The present findings indicate that enhanced hippocampal TNF production alone is sufficient to induce chronic pain symptoms. Future studies would be of interest to determine whether unilateral TNF nanoplasmidex microinjection produces similar changes within each hippocampus as well as in regards to ipsilateral versus contralateral peripheral hypersensitivity.

This study demonstrates that stereotaxic injection of TNF nanoplasmidexes into the brain, specifically into the hippocampus can effectively enhance TNF gene expression locally resulting in development of chronic pain behaviors. While nanoplasmidex expression of RFP and immunofluorescence labeling with anti-GFAP and anti-NF-200 antibodies indicates that either glial cells or neurons, respectively, are capable of being transfected and thereby producing TNF, the finding that enhanced TNF production restricted to the hippocampus is sufficient for inducing chronic pain behaviors is novel. These results reveal not only the pivotal role that a specific pleiotropic cytokine solely in the hippocampus plays in the development of chronic, persistent pain, but also suggests that this experimental paradigm may produce an animal model for chronic pain. In conclusion, all of the data presented herein in combination with previously published findings demonstrates a causative role for TNF specifically within the hippocampus in the pathogenesis of chronic pain as shown at the behavioral, physiological and cellular levels.

## Acknowledgments

This work was supported by the Department of Pathology and Anatomical Sciences, University at Buffalo School of Medicine and Biomedical Sciences, in partial fulfillment of the MA degree in Pathology (RTM) and from NIH grants: HL048889 (PRK, BAD) and AI084410 (PRK, BAD). NanoAxis, LLC positions that were served in an unpaid capacity during the undertaking of this research are as follows: Research Development Directors (RNS, TAI) and Scientific Advisory Board Members (PRK, PNP). We acknowledge the assistance of the Confocal Microscope and Flow Cytometry Facility in the School of Medicine and Biomedical Sciences, University at Buffalo.

## References

1. Acton J, McKenna JE, Melzack R. Amitriptyline produces analgesia in the formalin pain test. Exp Neurol. 1992; 117:94–96. [PubMed: 1618291]
2. Ahmed M, Deng Z, Narain R. Study of transfection efficiencies of cationic glyconanoparticles of different sizes in human cell line. ACS Appl Mater Interf. 2009; 1:1980–1987.
3. Aloisi AM. Sex differences in pain-induced effects on the septo-hippocampal system. Brain Res Rev. 1997; 25:397–406. [PubMed: 9495566]
4. Banks WA, Moinuddin A, Morley JE. Regional transport of TNF-alpha across the blood-brain barrier in young ICR and young and aged SAMP8 mice. Neurobiol Aging. 2001; 22:671–676. [PubMed: 11445267]
5. Berridge MV, Herst PM, Tan AS. Tetrazolium dyes as tools in cell biology: new insights into their cellular reduction. Biotechnol Annu Rev. 2005; 11:127–152. [PubMed: 16216776]
6. Bharali DJ, Klejbor I, Stachowiak EK, Dutta P, Roy I, Kaur N, Bergey EJ, Prasad PN, Stachowiak MK. Organically modified silica nanoparticles: a nonviral vector for *in vivo* gene delivery and expression in the brain. Proc Natl Acad Sci USA. 2005; 102:11539–11544. [PubMed: 16051701]
7. Bonoiu AC, Bergey EJ, Ding H, Hu R, Kumar R, Yong K-T, Prasad PN, Mahajan SD, Picchione KE, Bhattacharjee A, Ignatowski TA. Gold nanorod-siRNA induces efficient *in vivo* gene silencing in the rat hippocampus. Nanomedicine. 2011; 6:617–630. [PubMed: 21718174]
8. Bonoiu AC, Mahajan SD, Ding H, Roy I, Yong K-T, Kumar R, Hu R, Bergey EJ, Schwartz SA, Prasad PN. Nanotechnology approach for drug addiction therapy: Gene silencing using delivery of gold nanorod-siRNA nanoplex in dopaminergic neurons. Proc Natl Acad Sci USA. 2009; 106:5546–5550. [PubMed: 19307583]
9. Botney M, Fields HL. Amitriptyline potentiates morphine analgesia by a direct action on the central nervous system. Ann Neurol. 1983; 13:160–164. [PubMed: 6219612]
10. Bremner JD, Narayan M, Anderson ER, Staib LH, Miller HL, Charney DS. Hippocampal volume reduction in major depression. J Psychiatry. 2000; 157:115–118.
11. Bustin SA. Quantification of mRNA using real-time reverse transcription PCR (RT-PCR): trends and problems. J Mol Endocrinol. 2002; 1:23–39. [PubMed: 12200227]

12. Ceccarelli I, Scaramuzzino A, Aloisi AM. Effects of formalin pain on hippocampal c-fos expression in male and female rats. Pharmacol Biochem Behav. 1999; 64:797–802. [PubMed: 10593203]
13. Chakravarthy KV, Bonoiu AC, Davis WG, Ranjan P, Ding H, Hu R, Bowzard JB, Bergey EJ, Katz JM, Knight PR, Sambhara S, Prasad PN. Gold nanorod delivery of an ssRNA immune activator inhibits pandemic H1N1 influenza viral replication. Proc Natl Acad Sci USA. 2010; 107:10172–10177. [PubMed: 20498074]
14. Chaplan SR, Bach FW, Pogrel JW, Chung JM, Yaksh TL. Quantitative assessment of tactile allodynia in the rat paw. J Neurosci Meth. 1994; 53:55–63.
15. Chomczynski P, Sacchi N. Single-step method of RNA isolation by acid guanidinium thiocyanate-phenol-chloroform extraction. Anal Biochem. 1987; 162:156–159. [PubMed: 2440339]
16. Chou C-W, Wong GTC, Lim G, McCabe MF, Wang S, Irwin MG, Mao J. Peripheral nerve injury alters the expression of NF-κB in the rat's hippocampus. Brain Res. 2011; 1378:66–71. [PubMed: 21223950]
17. Cliffer K, Burstein R, Giesler G. Distribution in the hypothalamus and telencephalon of fibers originating in the spinal cord. Soc Neurosci Abs. 1988; 14:121.
18. Connor EE, Mwamuka J, Gole A, Murphy CJ, Wyatt MD. Gold nanoparticles are taken up by human cells but do not cause acute cytotoxicity. Small. 2005; 1:325–327. [PubMed: 17193451]
19. Covey WC, Ignatowski TA, Knight PR, Spengler RN. Brain-derived TNFα: involvement in neuroplastic changes implicated in the conscious perception of persistent pain. Brain Res. 2000; 859:113–122. [PubMed: 10720620]
20. Covey WC, Ignatowski TA, Renauld AE, Knight PR, Nader D, Spengler RN. Expression of neuron-associated tumor necrosis factor alpha in the brain is increased during persistent pain. Reg Anesth Pain Med. 2002; 27:357–366. [PubMed: 12132059]
21. Cunha FQ, Poole S, Lorenzetti B, Ferreira S. The pivotal role of tumor necrosis factor alpha in the development of inflammatory hyperalgesia. Br J Pharmacol. 1992; 107:660–664. [PubMed: 1472964]
22. Deleo JA, Colburn RW, Rickman AJ. Cytokine and growth factor immunohistochemical spinal profiles in two animal models of mononeuropathy. Brain Res. 1997; 759:50–57. [PubMed: 9219862]
23. Derbyshire SW, Jones AK, Gyulai F, Clark S, Townsend D, Firestone LL. Pain processing during three levels of noxious stimulation produces differential patterns of central activity. Pain. 1997; 73:431–445. [PubMed: 9469535]
24. Ding H, Yong K-T, Roy I, Pudavar HE, Law WC, Bergey EJ, Prasad PN. Gold nanorods coated with multilayer polyelectrolyte as contrast agents for multimodal imaging. J Phys Chem C. 2007; 111:12552–12557.
25. Duric V, McCarson KE. Effects of analgesic or antidepressant drugs on pain- or stress-evoked hippocampal and spinal neurokinin-1 receptor and brain-derived neurotrophic factor gene expression in the rat. J Pharmacol. 2006; 319:1235–1243.
26. Duric V, McCarson KE. Neurokinin-1 (NK-1) receptor and brain-derived neurotrophic factor (BDNF) gene expression is differentially modulated in the rat spinal dorsal horn and hippocampus during inflammatory pain. Mol Pain. 2007; 3:32–39. [PubMed: 17974009]
27. Duric V, McCarson KE. Persistent pain produces stress-like alterations in hippocampal neurogenesis and gene expression. J Pain. 2006; 7:544–555. [PubMed: 16885011]
28. Dutar P, Lamour Y, Jobert A. Activation of indentified septo-hippocampal neurons by noxious peripheral stimulation. Brain Res. 1985; 328:15–21. [PubMed: 3971172]
29. Dworkin RH, Gitlin MJ. Clinical aspects of depression in chronic pain patients. Pain. 1991; 7:79–94.
30. Emad Y, Ragab Y, Zeinhom F, El-Khouly G, Abou-Zeid A, Rasker JJ. Hippocampus dysfunction may explain symptoms of fibromyalgia syndrome. A study with single-voxel magnetic resonance spectroscopy. J Rheumatol. 2008; 35:1371–1377. [PubMed: 18484688]
31. Eskandari MK, Nguyen DT, Kunkel SL, Remick DG. WEHI 164 subclone 13 assay for TNF: sensitivity, specificity, and reliability. Immunol Invest. 1990; 19:69–79. [PubMed: 2110931]

32. Francischi JN, Yokoro CM, Poole S, Tafuri WL, Cunha FQ, Teixeira MM. Anti-inflammatory and analgesic effects of the phosphodiesterase 4 inhibitor rolipram in a rat model of arthritis. J Pharmacol. 2000; 399:243–249.
33. Greten TF, Eigler A, Sinha B, Moeller J, Endres S. The specific type IV phosphodiesterase inhibitor rolipram differentially regulates the proinflammatory mediators TNF-alpha and nitric oxide. Int J Immunopharmacol. 1995; 17:605–610. [PubMed: 8586489]
34. Hargreaves K, Dubner R, Brown F, Flores C, Joris J. A new and sensitive method for measuring thermal nociception in cutaneous hyperalgesia. Pain. 1988; 32:77–88. [PubMed: 3340425]
35. Hauck TS, Ghazani AA, Chan WC. Assessing the effect of surface chemistry on gold nanorod uptake, toxicity, and gene expression in mammalian cells. Small. 2008; 4:153–159. [PubMed: 18081130]
36. Herpfer I, Hunt SP, Stanford SC. A comparison of neurokinin 1 receptor knockout (NK1-/-) and wildtype mice: exploratory behaviour and extracellular noradrenaline concentration in the cerebral cortex of anaesthetised subjects. Neuropharmacology. 2005; 48:706–719. [PubMed: 15814105]
37. Ignatowski TA, Covey WC, Knight PR, Severin CM, Nickola TJ, Spengler RN. Brain-derived TNF mediates neuropathic pain. Brain Res. 1999; 841:70–77. [PubMed: 10546989]
38. Ignatowski TA, Noble BK, Wright JR, Gorfien J, Heffner RR, Spengler RN. Neuronal-associated tumor necrosis factor (TNF : its role in noradrenergic functioning and modification of its expression following antidepressant drug administration. J Neuroimmunol. 1997; 79:84–90. [PubMed: 9357451]
39. Ignatowski TA, Reynolds JL, Sud R, Knight PR, Spengler RN. The dissipation of neuropathic pain paradoxically involves the presence of tumor necrosis factor-(TNF). Neuropharmacology. 2005; 48:448–460. [PubMed: 15721177]
40. Ignatowski TA, Spengler RN. Tumor Necrosis Factor- : presynaptic sensitivity is modified after antidepressant drug administration. Brain Res. 1994; 665:293–299. [PubMed: 7895065]
41. Khabar KSA, Siddiqui S, Armstrong JA. WEHI-13VAR: a stable and sensitive variant of WEHI 164 clone 13 fibrosarcoma for tumor necrosis factor bioassay. Immunol Lett. 1995; 46:107–110. [PubMed: 7590904]
42. Khanna S, Sinclair JG. Noxious stimuli produce prolonged changes in the CA1 region of the rat hippocampus. Pain. 1989; 39:337–343. [PubMed: 2616183]
43. Klejbor I, Stachowiak EK, Bharali DJ, Roy I, Spodnik I, Morys J, Bergey EJ, Prasad PN, Stachowiak MK. ORMOSIL nanoparticles as a non-viral gene delivery vector for modeling polygltamine induced brain pathology. J Neurosci Meth. 2007; 165:230–243.
44. Lindvall, O.; Bjorklund, A. Organization of catecholamine neurons in the rat central nervous system. Plenum Press; New York, NY: 1978. p. 139
45. McEwen BS. Plasticity of the hippocampus: adaptation to chronic stress and allostatic load. Ann NY Acad Sci. 2001; 933:265–277. [PubMed: 12000027]
46. McEwen BS, Magarinos AM. Stress and hippocampal plasticity: implications for the pathophysiology of affective disorders. Hum Psychopharmacol. 2001; 16:S7–S19. [PubMed: 12404531]
47. McKenna JE, Melzack R. Analgesia produced by lidocaine microinjection into the dentate gyrus. Pain. 1992; 49:105–112. [PubMed: 1594270]
48. Ohtori S, Takahashi K, Moriya H, Myers RR. TNF-alpha and TNF-alpha receptor type 1 upregulation in glia and neurons after peripheral nerve injury: studies in murine DRG and spinal cord. Spine. 2004; 29:1082–1088. [PubMed: 15131433]
49. Oka T, Wakugawa Y, Hosoi M, Oka K, Hori T. Intracerebroventricular injection of tumor necrosis factor-alpha induces thermal hyperalgesia in rats. Neuroimmunomodulation. 1996; 3:135–140. [PubMed: 8945729]
50. Pan W, Kastin AJ, Daniel J, Yu C, Baryshnikova LM, von Bartheld CS. TNFalpha trafficking in cerebral vascular endothelial cells. J Neuroimmunology. 2007; 185:47–56. [PubMed: 17316829]
51. Paxinos, G.; Watson, C. The rat brain in stereotaxic coordinates. Academic Press; New York: 1997.

52. Radonic A, Thulke S, Mackay IM, Landt O, Siegert W, Nitsche A. Guideline to reference gene selection for quantitative real-time PCR. Biochem Biophys Res Commun. 2004; 313:856–862. [PubMed: 14706621]
53. Reeve AJ, Patel S, Fox A, Walker K, Urban L. Intrathecally administered endotoxin or cytokines produce allodynia, hyperalgesia and changes in spinal cord neuronal responses to nociceptive stimuli in the rat. Eur J Pain. 2000; 4:247–257. [PubMed: 10985868]
54. Reynolds JL, Ignatowski TA, Sud R, Spengler RN. An antidepressant mechanism of desipramine is to decrease TNF production culminating in increases in noradrenergic neurotransmission. Neuroscience. 2005; 133:519–531. [PubMed: 15878644]
55. Reynolds JL, Ignatowski TA, Sud R, Spengler RN. Brain-derived tumor necrosis factor-alpha and its involvement in noradrenergic neuron functioning in the mechanism of action of an antidepressant. J Pharmacol Exp Ther. 2004; 310:1216–1225. [PubMed: 15082752]
56. Richelson E, Pfenning M. Blockade by antidepressants and related compounds of biogenic amine uptake into rat brain synaptosomes: most antidepressants selectively block norepinephrine uptake. Eur J Pharmacol. 1984; 104:277–286. [PubMed: 6499924]
57. Roy I, Stachowiak MK, Bergey EJ. Non viral gene transfection nanoparticles: Functions and applications in CNS. Nanomedicine. 2008; 4:89–97. [PubMed: 18313990]
58. Ruifrok AC, Johnston DA. Quantification of histochemical staining by color deconvolution. Anal Quant Cytol Histol. 2001; 23:291–299. [PubMed: 11531144]
59. Sacerdote P, Brini A, Mantegazza P, Panerai AE. A role for serotonin and beta-endorphin in the analgesia induced by some tricyclic antidepressant drugs. Biochem Pharmacol. 1987; 26:153–158.
60. Santarelli L, Saxe M, Gross C, Surget A, Battaglia F, Dulawa S, Weisstaub N, Lee J, Duman R, Arancio O, Belzung C, Hen R. Requirement of hippocampal neurogenesis for the behavioral effects of antidepressant. Science. 2003; 301:805–809. [PubMed: 12907793]
61. Schafers M, Svensson CI, Sommer C, Sorkin LS. Tumor necrosis factor-alpha induces mechanical allodynia after spinal nerve ligation by activation of p38 MAPK in primary sensory neurons. J Neurosci. 2003; 23:2517–2521. [PubMed: 12684435]
62. Sheline YI, Gado MH, Kraemer HC. Untreated depression and hippocampal volume loss. Am J Psychiatry. 2003; 160:1516–1518. [PubMed: 12900317]
63. Soleimannejad E, Naghdi N, Semnanian S, Fathollahi Y, Kazemnejad A. Antinociceptive effect of intra-hippocampal CA1 and dentate gyrus injection of MK801 and AP5 in the formalin test in adult male rats. Eur J Pharmacol. 2006; 562:39–46. [PubMed: 17362915]
64. Sommer C, Marziniak M, Myers RR. The effect of thalidomide treatment on vascular pathology and hyperalgesia caused by chronic constriction injury of rat nerve. Pain. 1998; 74:83–91. [PubMed: 9514564]
65. Sommer C, Myers RR. Thalidomide inhibition of TNF reduces hyperalgesia in neuropathic rats. Reg Anesth. 1994; 19:1. [PubMed: 8204558]
66. Sommer C, Schmidt C, George A, Toyka KV. A metalloprotease-inhibitor reduces pain-associated behavior in mice with experimental neuropathy. Neurosci Lett. 1997; 237:45–48. [PubMed: 9406876]
67. Sommer N, Loschmann PA, Northoff GH, Weller M, Steinbrechter A, Steinbach JP, Lichtenfels R, Meyermann R, Riethmuller A, Fontana A, Dichgans J, Martin R. The antidepressant rolipram suppresses cytokine production and prevents autoimmune encephalomyelitis. Nat Med. 1995; 1:244–248. [PubMed: 7585041]
68. Spengler RN, Sud R, Knight PR, Ignatowski TA. Antinociception mediated by $_2$-adrenergic activation involves increasing tumor necrosis factor alpha (TNF ) expression and restoring TNF and $_2$-adrenergic inhibition of norepinephrine release. Neuropharmacology. 2007; 52:576–589. [PubMed: 17055005]
69. Starke K. Regulation of noradrenaline release by presynaptic receptor systems. Rev Physiol Biochem Pharmacol. 1977; 77:1–124. [PubMed: 14389]
70. Sud R, Ignatowski TA, Lo CPK, Spengler RN. Uncovering molecular elements of brain-body communication during development and treatment of neuropathic pain. Brain Behav Immun. 2007; 21:112–124. [PubMed: 16859892]

71. Sud R, Spengler RN, Nader DN, Ignatowski TA. Antinociception occurs with a reversal in $_2$-adrenoceptor regulation of TNF production by peripheral monocytes/macrophages from pro- to anti-inflammatory. Eur J Pharmacol. 2008; 588:217–231. [PubMed: 18514187]

72. Suzuki R, Morcuende S, Webber M, Hunt SP, Dickenson AH. Superficial NK1-expressing neurons control spinal excitability through activation of descending pathways. Nat Neurosci. 2002; 5:1319–1326. [PubMed: 12402039]

73. Wagner R, Myers RR. Endoneurial injection of TNF-alpha produces neuropathic pain behaviors. Neuroreport. 1996; 7:2897–2901. [PubMed: 9116205]

74. Watkins LR, Wiertelak EP, Goehler LE, Smith KP, Martin D, Maier SF. Characterization of cytokine-induced hyperalgesia. Brain Res. 1994; 654:15–26. [PubMed: 7982088]

75. Wei F, Xu ZC, Qu Z, Milbrandt J, Zhou M. Role of EGR1 in hippocampal synaptic enhancement induced by tetanic stimulation and amputation. J Cell Biol. 2000; 149:1325–1334. [PubMed: 10871275]

76. Xu JT, Xin WJ, Zang Y, Wu CY, Liu XG. The role of tumor necrosis factor-alpha in the neuropathic pain induced by lumbar 5 ventral root transection in rat. Pain. 2006; 123:306–321. [PubMed: 16675114]

77. Yong K-T, Roy I, Ding H, Bergey EJ, Prasad PN. Biocompatible near-infrared quantum dots as ultrasensitive probes for long-term *in vivo* imaging applications. Small. 2009; 5:1997–2004. [PubMed: 19466710]

78. Yong K-T, Sahoo Y, Swihart MT, Schneeberger PM, Prasad PN. Templated synthesis of gold nanorods (NRs): The effects of cosurfactants and electrolytes on the shape and optical properties. Top Catal. 2008; 47:49–60.

79. Zelenka M, Schafers M, Sommer C. Intraneural injection of interleukin-1beta and tumor necrosis factor-alpha into rat sciatic nerve at physiological doses induces signs of neuropathic pain. Pain. 2005; 116:257–263. [PubMed: 15964142]

80. Zimmermann M. Ethical guidelines for investigations of experimental pain in conscious animals. Pain. 1983; 16:109–110. [PubMed: 6877845]

## Summary

Increasing only the expression of the pleiotropic cytokine tumor necrosis factor-alpha exclusively in the hippocampus of naïve rats induces peripheral hypersensitivity to thermal and mechanical stimulation reminiscent of chronic pain behaviors.

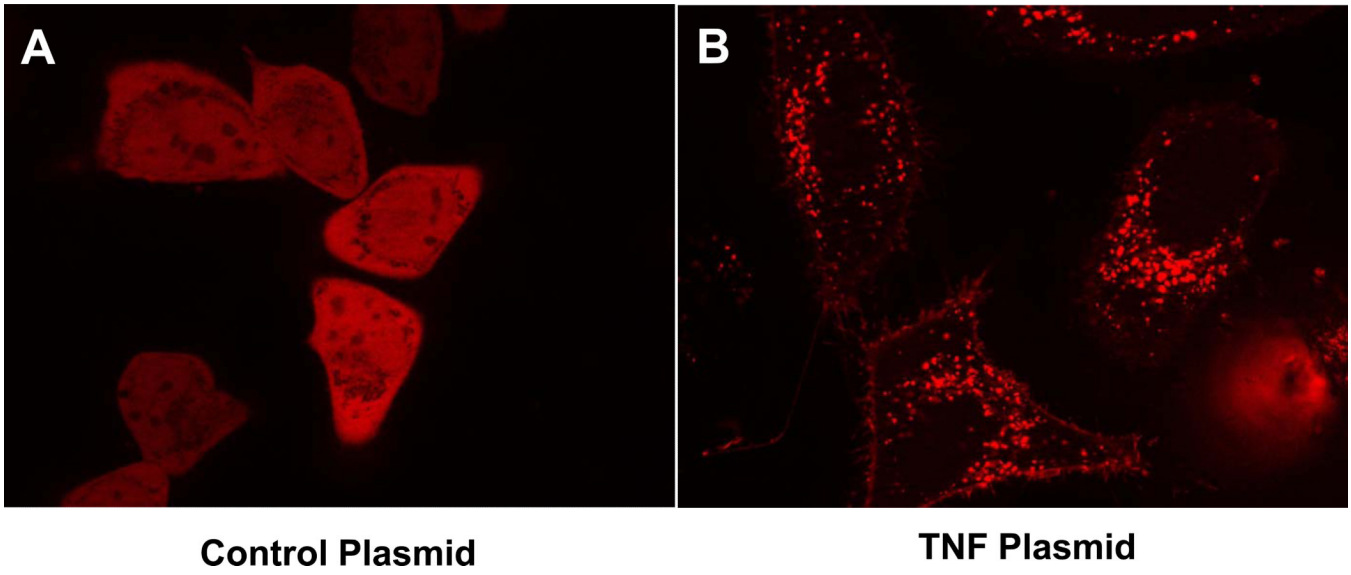


**Figure 1.**

HeLa cells were transfected with (**A**) pTag*rfp*-C, or (**B**) pTag*rfp*-Mu*tnf* using FuGENE HD as a transfection agent. The cells were imaged 72 hours later using the Zeiss Axio Observer Inverted Microscope with dsRed filter set. The pTag*rfp*-C transfected cells demonstrate homogenous cytosolic distribution of RFP, whereas the pTag*rfp*-Mu*tnf* transfected cells demonstrate heterogenous, punctate fluorescence associated with the Golgi apparatus, vesiclular packaging, and plasma membrane insertion of RFP-MuTNF fusion protein.

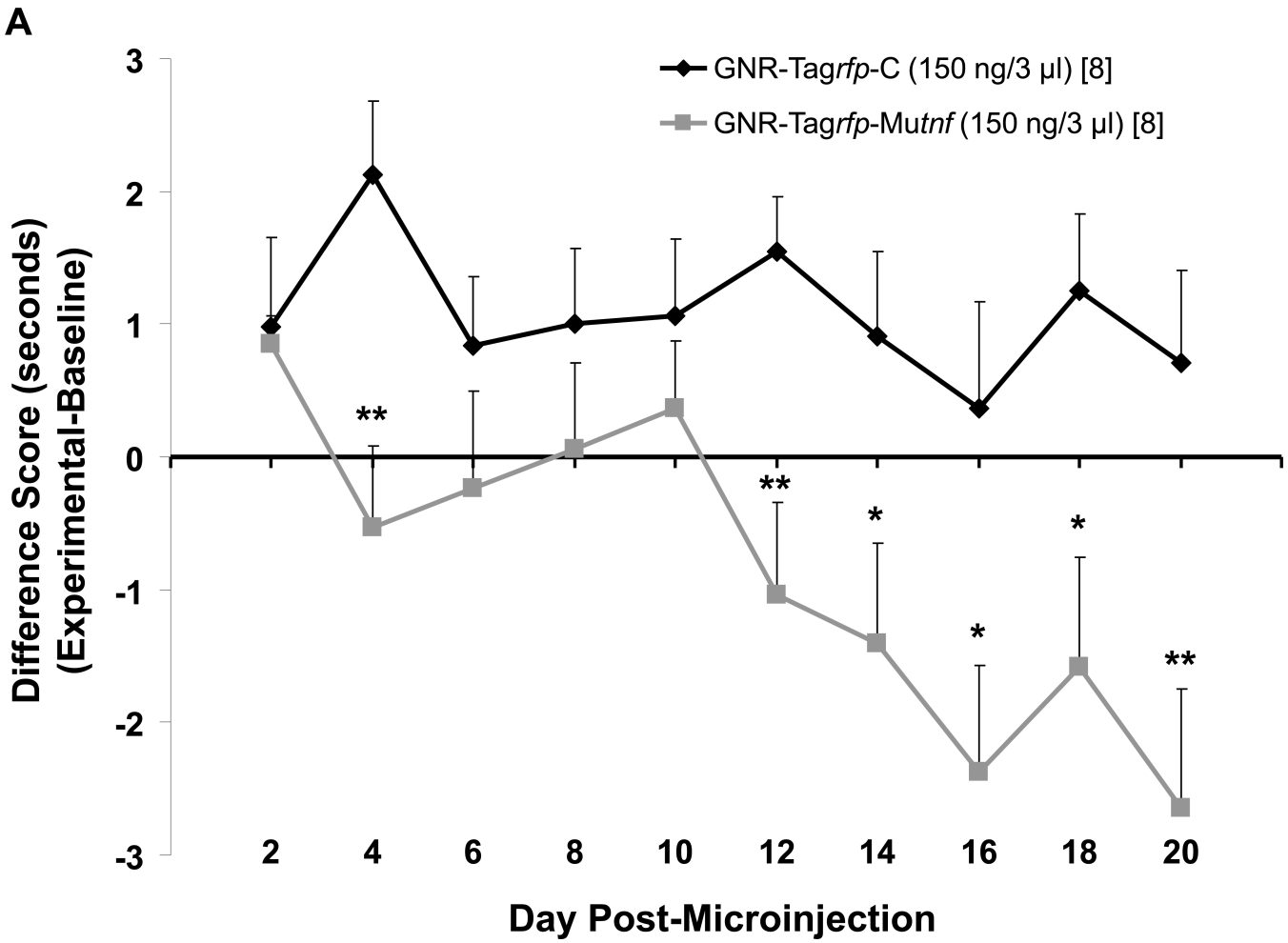

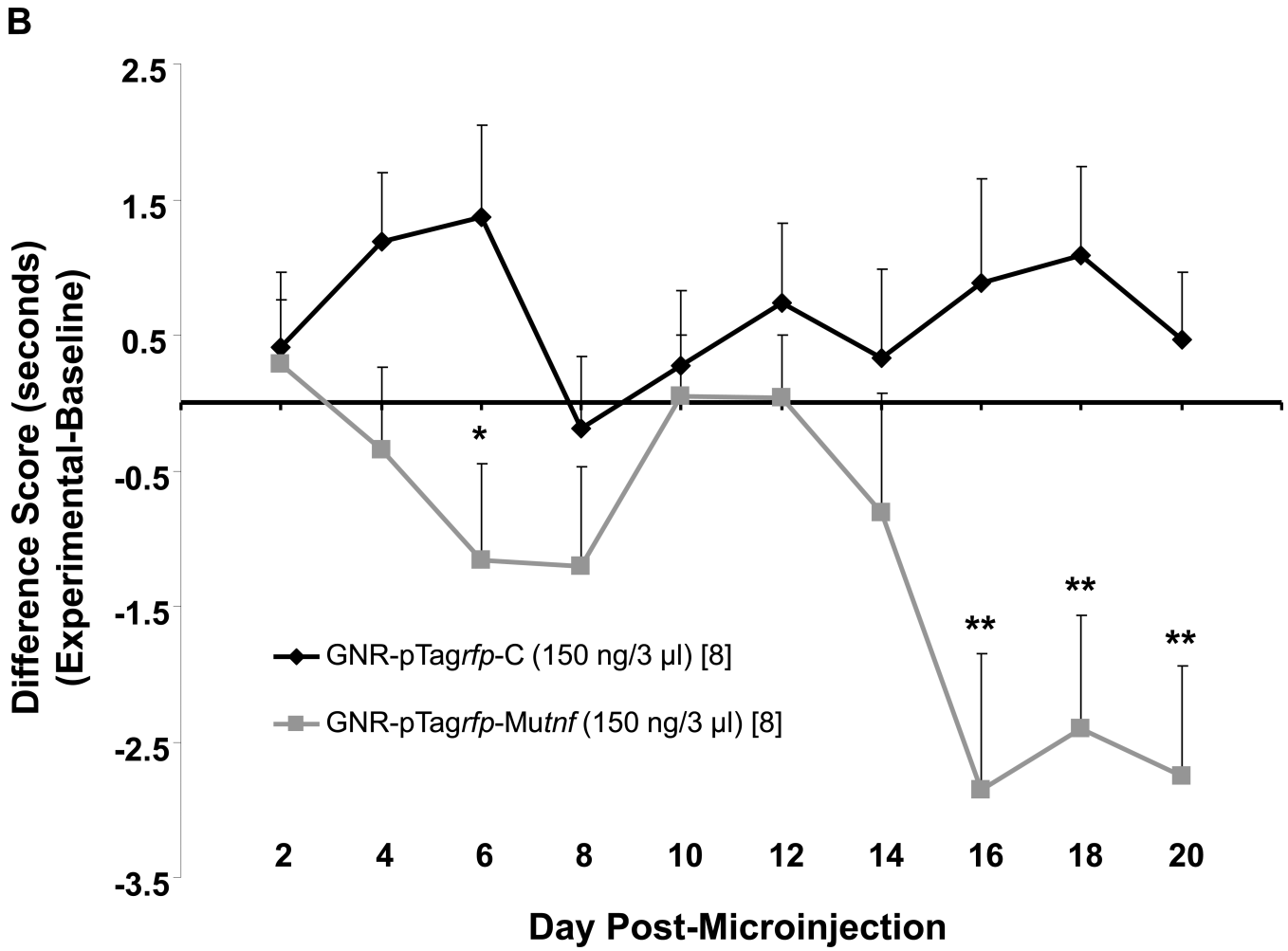


**Figure 2.**

Sprague-Dawley rats (250–300 g) microinjected with 150 ng/3 µl GNR-pTag*rfp*-Mu*tnf* nanoplasmidexes bilaterally into the hippocampal CA1 region develop thermal hyperalgesia. Data are presented as the difference score of (**A**) right hind paw or (**B**) left hind paw experimental (post-microinjection) – hind paw baseline withdrawal latencies in seconds. Each point is expressed as the mean ± S.E.M. (number of rats in brackets). Statistical significance different from GNR-pTag*rfp*-C control nanoplasmidex microinjected rats was reached at * $p < 0.05$, ** $p \leq 0.01$ using a Student's *t*-test. Baseline [n = 16] withdrawal latencies averaged 12.8 ± 0.4 s for the right hind paw and 13.2 ± 0.3 s for the left hind paws.

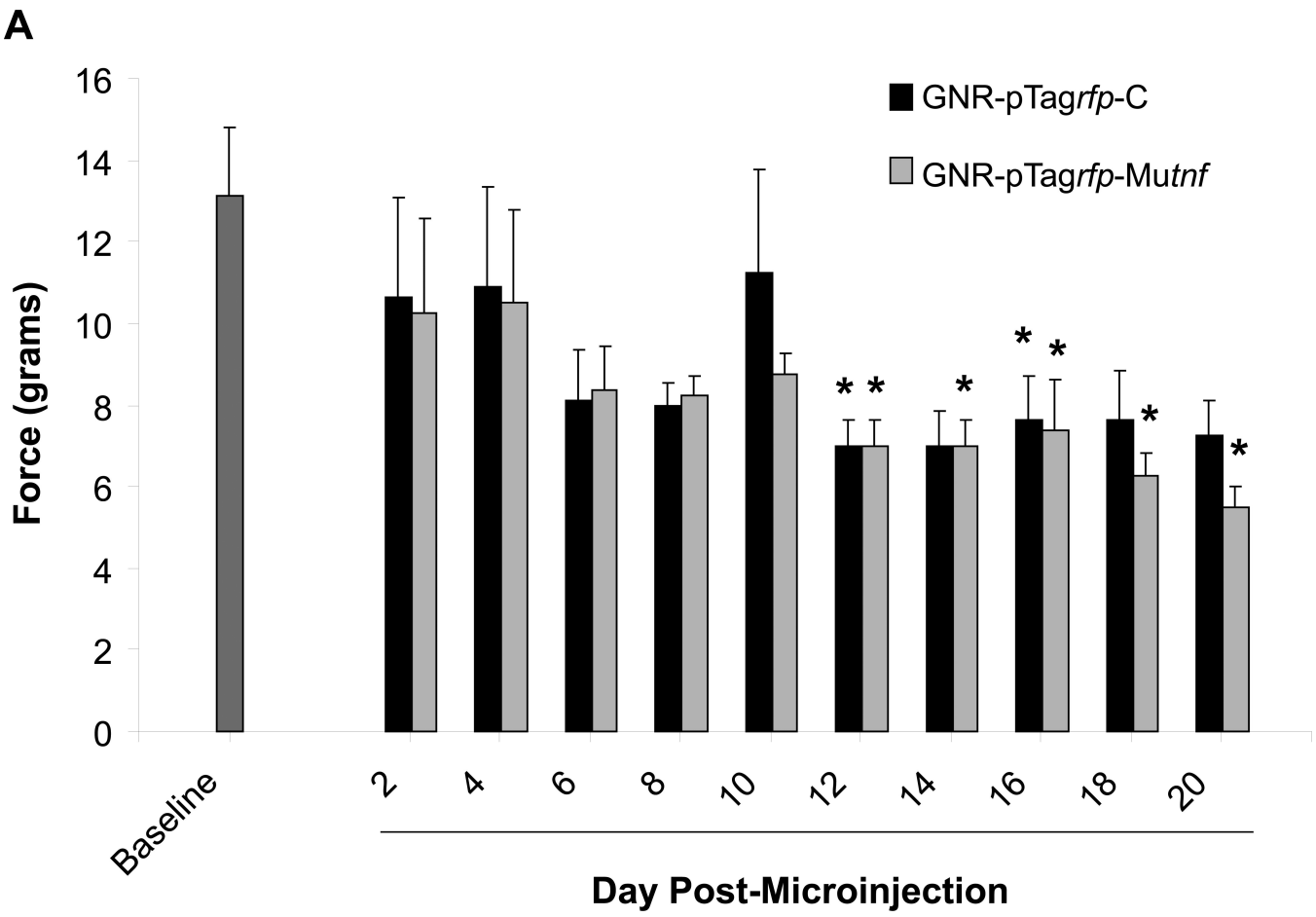

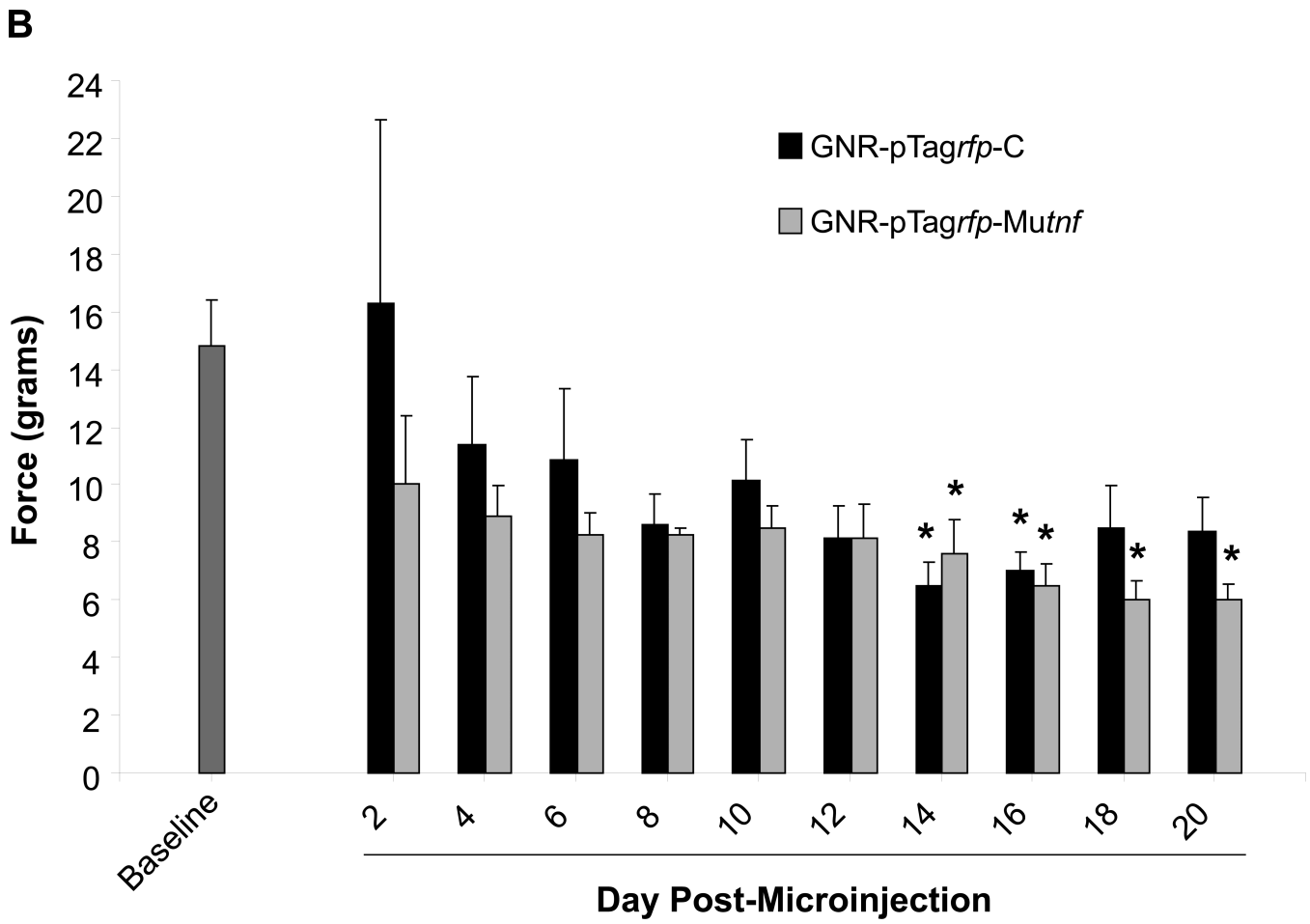


**Figure 3.**

Development of sensitivity to mechanical stimulation by von Frey hairs in animals receiving GNR-pTag*rfp*-Mu*tnf* nanoplasmidexes into the CA1 region of the hippocampus. Mechanical sensitivity/allodynia was determined by measuring the paw withdrawal threshold every other day post-surgery and comparing to the baseline (the measurements taken over 3 days prior to surgery) values. (**A**) Right hind paw withdrawal thresholds expressed as grams of force (mean ± S.E.M., n = 8); (**B**) Left hind paw withdrawal thresholds (mean ± S.E.M., n = 8). * $p < 0.05$ as compared with baseline, Kruskal-Wallis ANOVA on Ranks and Dunn's post-hoc test. **Note:** Allodynia responses are more consistently produced by rats microinjected with the GNR-pTag*rfp*-Mu*tnf* nanoplasmidexes.

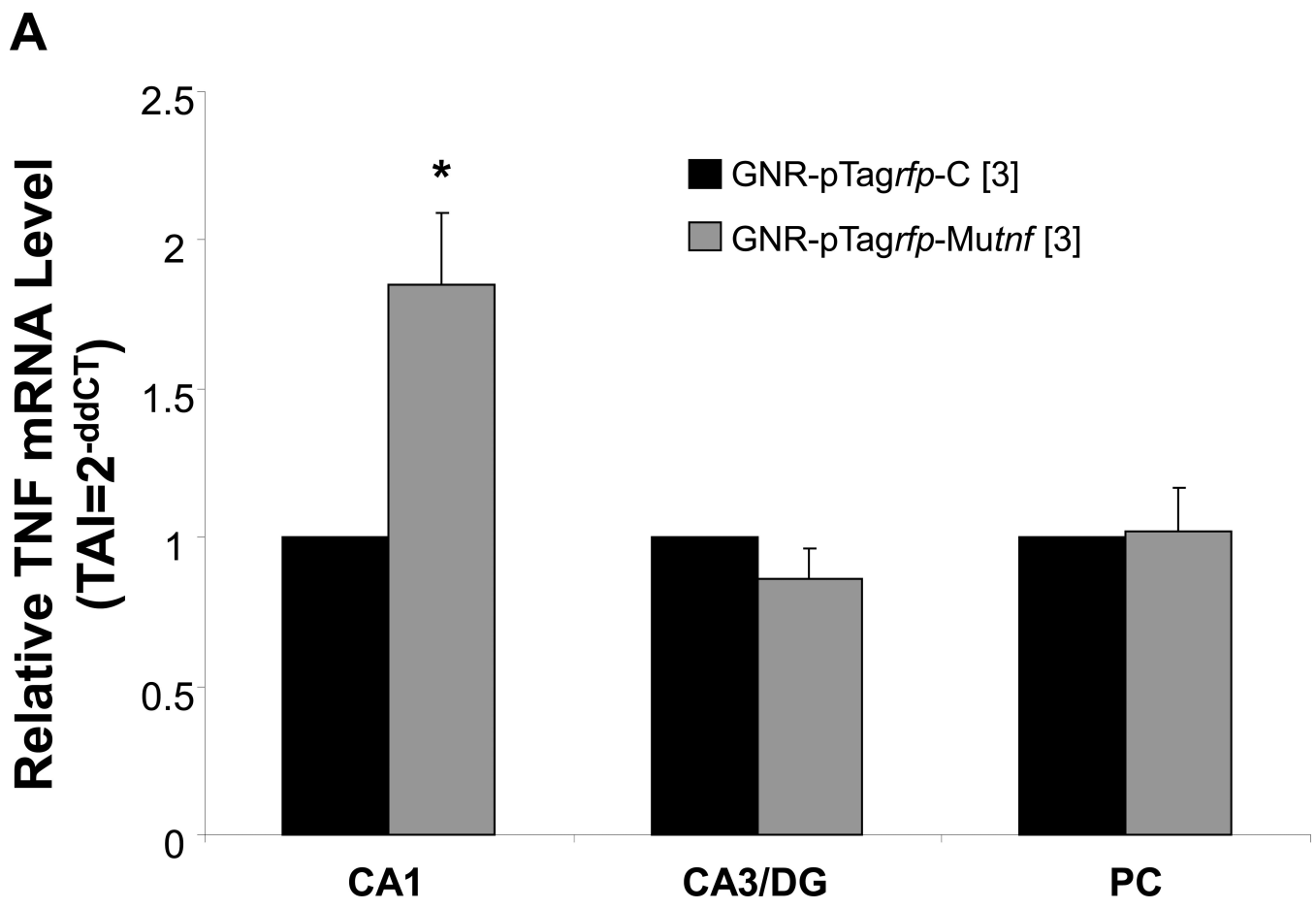

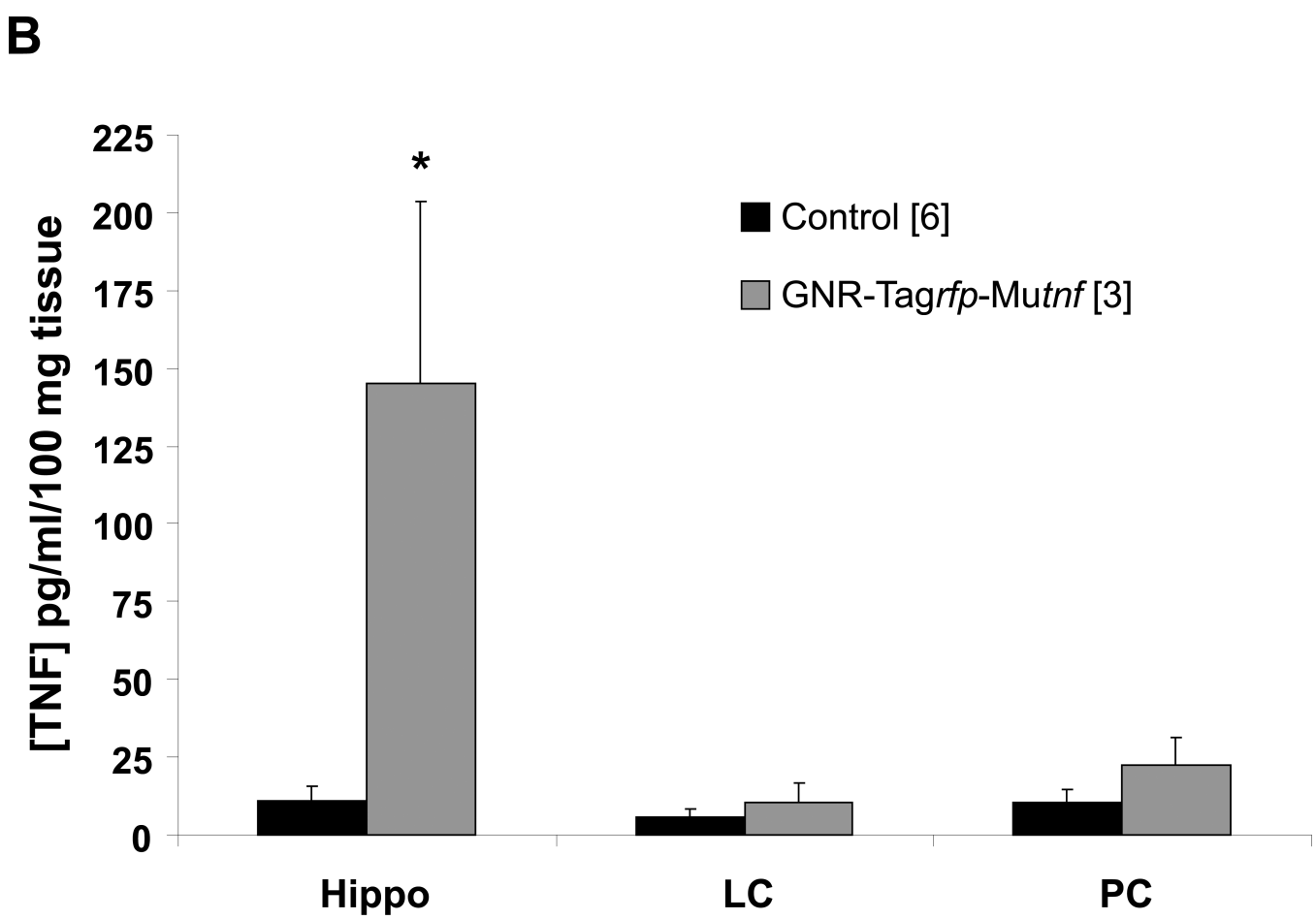


**Figure 4.**

Induction of (**A**) gene expression and (**B**) bioactive production of TNF 21 days after bilateral GNR-pTag*rfp*-Mu*tnf* nanoplasmidex (150 ng/3 μl) microinjection into the hippocampal CA1 region. Data in **A** represents the mean ± S.E.M. of three separate experiments. Statistical significance indicated (* $p < 0.05$) was by Student's *t*-test. CA1, left hippocampal CA1 region; CA3/DG, combined left hippocampal CA3/dentate gyrus regions; and PC, left parietal cortex. The Control group in **B** represents combined GNR-pTag*rfp*-C control nanoplasmidex (150 ng/3 μl) (n=3) and Control (naïve animals) (n=3) values, as there was no difference between the two groups. LC = locus coeruleus; PC = parietal cortex; both assayed as control regions to test for diffusion effects. Statistically significant from Control, * $p < 0.05$ ($p = 0.011$), Student's *t*-test.

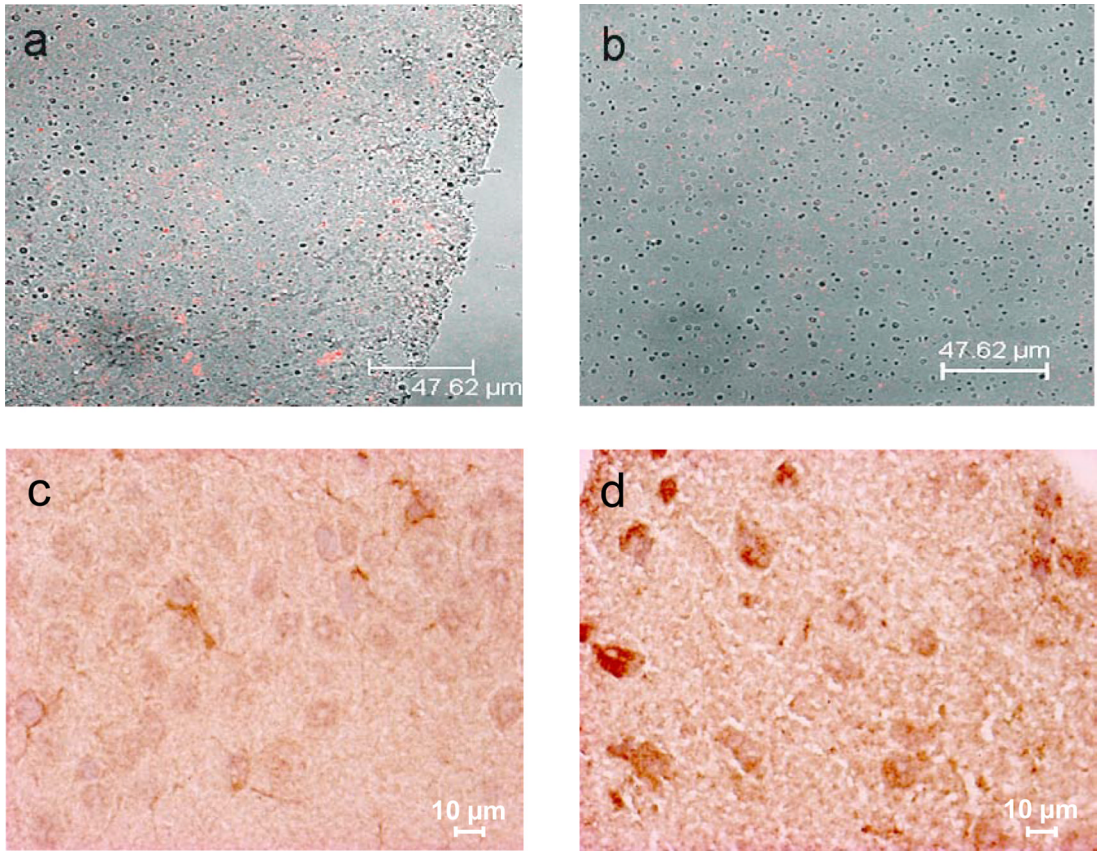


**Figure 5.**

Nanoplasmidex RFP distribution and immunohistochemical TNF staining in rat hippocampus. Confocal microscopic images of the CA1 region in right hippocampus sections (4-6 μm, unfixed) of rats 21 days after injection of nanoplasmidex (**a**) GNR-pTag*rfp*-C or (**b**) GNR-pTag*rfp*-Mu*tnf* (150 ng/3 μl). Panels **a** and **b** display fluorescence images acquired with a 590 nm filter overlaid with transmission images. Red indicates RFP generated by transcription/translation of pTag*rfp* in successfully transfected hippocampal cells. Injection of GNRs alone results in absence of fluorescence (data not shown); injection of pTag*rfp*-C construct alone demonstrates staining that is of less intensity and more diffuse (not cellularly localized; data not shown). Nanoplasmidex distribution data are representative of three separate experiments. Panels **c** and **d** are representative coronal hippocampal sections prepared from individual rats (at day-21 post-microinjection) receiving bilateral CA1 hippocampal microinjection of nanoplasmidexes (150 ng/3 ul). Sections are from paired rats receiving either (**c**) GNR-pTag*rfp*-C (control) nanoplasmidex or (**d**) GNR-pTag*rfp*-Mu*tnf* (TNF) nanoplasmidex. Note the increase in staining for TNF in panel **d** representing tissue from rats receiving the GNR-pTag*rfp*-Mu*tnf* nanoplasmidex microinjection. TNF staining data are representative of six individual experiments.

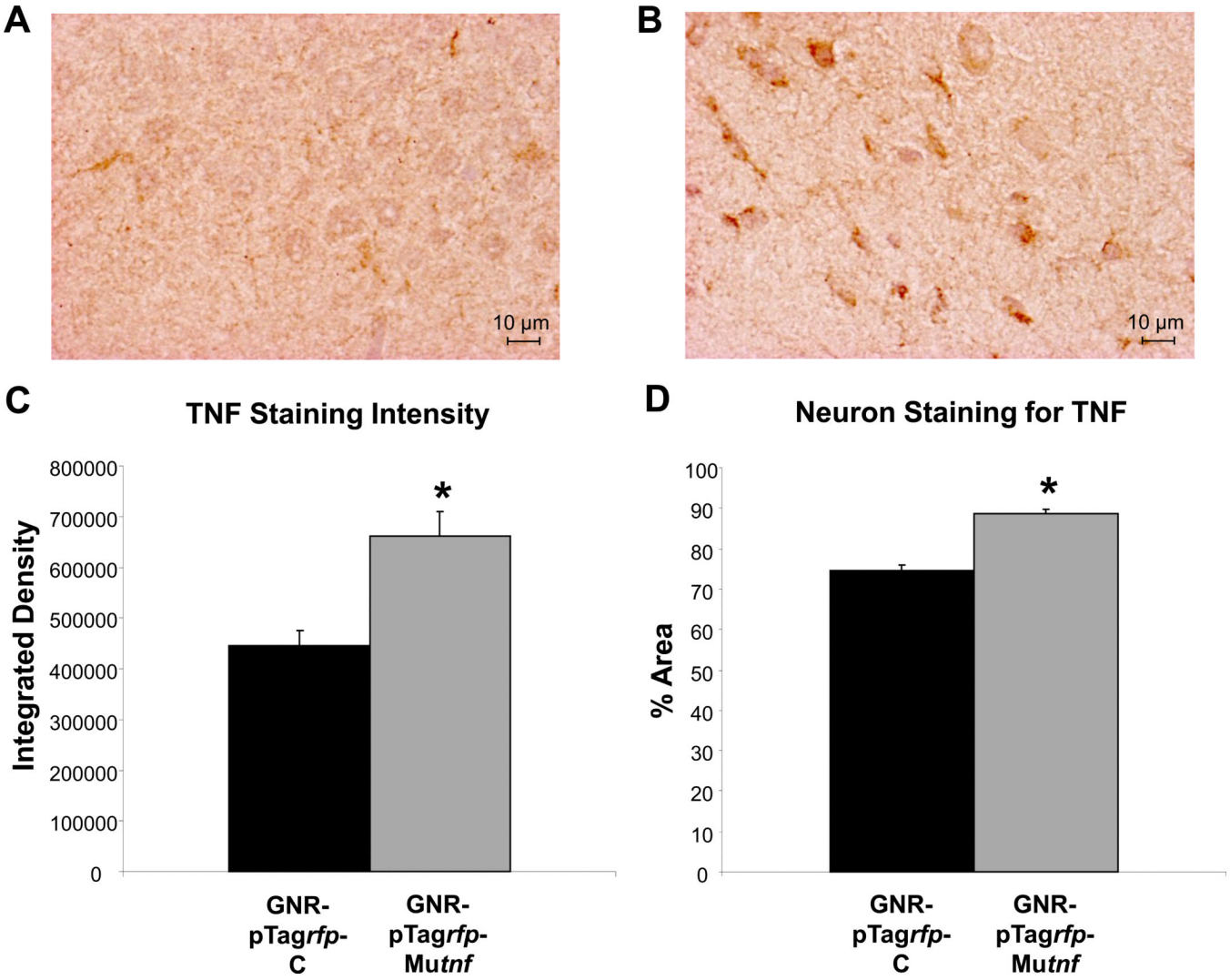


**Figure 6.**

Quantitative analysis of TNF immunoreactive staining. Representative coronal hippocampal sections from paired rats receiving either (**A**) GNR-pTag*rfp*-C (control) nanoplasmidex or (**B**) GNR-pTag*rfp*-Mu*tnf* (TNF) nanoplasmidex. (**C**) Statistical analysis of integrated density values (Mann-Whitney Rank Sum test) in hippocampal sections prepared from rats bilaterally microinjected with 150 ng/3 μl GNR-pTag*rfp*-Mu*tnf* nanoplasmidex into the CA1 region as compared to the hippocampus from GNR-pTag*rfp*-C control nanoplasmidex microinjected rats (* $p < 0.001$). (**D**) Statistical analysis of the % of the area of individual neurons ($n = 10$/high field (400X) area/section randomly chosen from 3 separate rats/group) that stained for TNF in hippocampal neurons from GNR-pTag*rfp*-Mu*tnf* nanoplasmidexes microinjected rats as compared to GNR-pTag*rfp*-C control nanoplasmidexes injected rats (* $p < 0.001$, Mann-Whitney Rank Sum test). Images were analyzed using ImageJ 1.32j software (NIH, USA, http://rsb.info.nih.gov/ij/) with the Color Deconvolution plug-in to perform stain separation (hematoxylin and DAB).

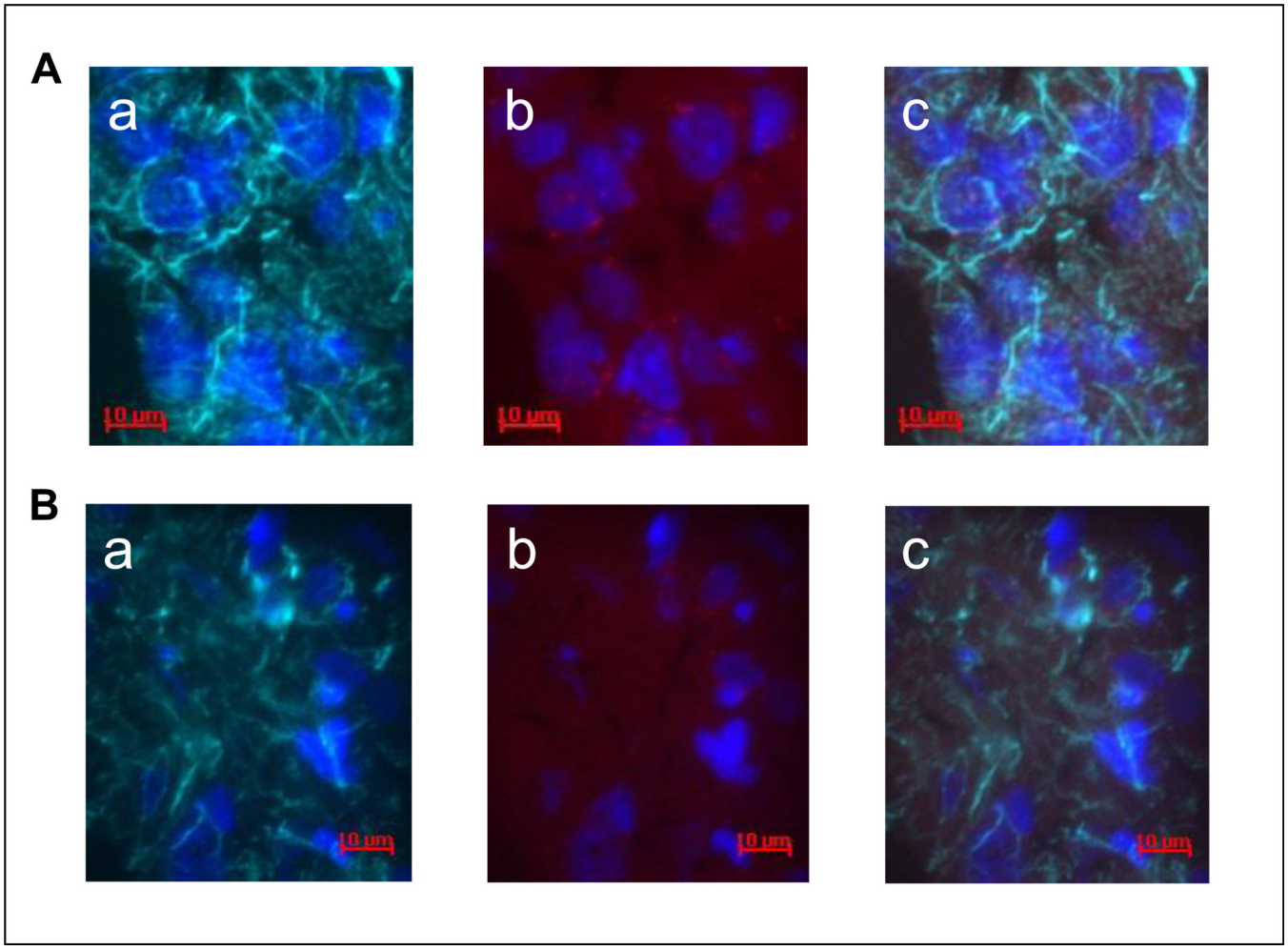


**Figure 7.**

Immunofluorescent labeling shows nanoplasmidex co-localization in rat coronal hippocampal sections. Nanoplasmidexes, which express RFP, were injected into the CA1 region of the hippocampus. The hippocampi were isolated 21 days later and frozen tissue sections were prepared. Identification of cell type was by immunofluorescent staining (4-6 μm section, acetone-fixed). **Row A:** Co-localization of RFP and NF-200 staining. Visualization of Neurofilament-200, NF-200 (1:30,000, Sigma) staining for neurons (Row **A**, panel a) using goat anti-mouse IgG1-AlexaFluor 647 (1:2,000, Invitrogen) secondary antibody (indicated as green) and nuclear (Hoechst dye, 10 μM) blue staining (panel a); GNR-pTag *rfp*-Mu*tnf* (TNF) nanoplasmidex staining (red) and nuclear blue staining (panel b); overlay of images (panel c) shows co-localization. **Row B:** Co-localization of RFP with GFAP staining. Glial fibrillary acidic protein, GFAP (1:30,000, Sigma-Aldrich) staining for glial cells (Row B, panel a) using goat anti-mouse IgG1-AlexaFluor 647 (1:2,000, Invitrogen) secondary antibody (green); GNR-pTag*rfp*-Mu*tnf* (TNF) nanoplasmidex staining (red) and nuclear blue staining (panel b); overlay of images (panel c) shows co-localization. Data is representative of three replicate experiments.